

TECHNICAL REPORT SIT-DL-06-9-2845

March, 2006

Inclusion of “Whisker Spray” Drag in
Performance Prediction Method
for High-Speed Planing Hulls

by

Daniel Savitsky
Michael F. DeLorme
and
Raju Datla

Prepared for:

The Society of Naval Architects and Marine
Engineers
Under Purchase Order Number: 5023

Presented at

Meeting of New York Metropolitan Section
The Society of Naval Architects and Marine
Engineers
March 14, 2006

(Davidson Laboratory Project No. 5656)

DAVIDSON LABORATORY
STEVENS INSTITUTE OF TECHNOLOGY
Castle Point Station
Hoboken, New Jersey 07030

Technical Report SIT-DL-06-9-2845

INCLUSION OF “WHISKER SPRAY” DRAG IN
PERFORMANCE PREDICTION METHOD
FOR HIGH-SPEED PLANING HULLS

By

Daniel Savitsky¹
Michael F. DeLorme²
and
Raju Datla³

Presented at
Meeting of New York Metropolitan Section
The Society of Naval Architects and Marine Engineers
March 14, 2006

(Davidson Laboratory Project: 5656)

-
1. Professor Emeritus, Davidson Laboratory, Stevens Institute of Technology
 2. Research Engineer, Davidson Laboratory, Stevens Institute of Technology
 3. Research Assistant Professor, Davidson Laboratory, Stevens Institute of Technology

ABSTRACT

The planing hull performance prediction method published by Savitsky in the October, 1964 issue of SNAME's Marine Technology included only the viscous drag and pressure drag components in the bottom area aft of the stagnation line. It did not include the viscous drag in the so-called "whisker spray" area forward of the stagnation line nor the aerodynamic drag of the hull cross-sectional area. To date the resistance component of the whisker spray has not been studied although it can become significant at high speed (estimated to be as much as 15% of the total drag). The present study fills this void and develops, for the first time, a method for quantifying the whisker spray contribution to total hull resistance as a function of deadrise angle, trim angle and speed and incorporates the results into the SNAME published hull performance prediction method. The analytical results are compared with data from model tests conducted at three separate towing tank facilities and show fairly good agreement with these data. In addition:

- Procedures are provided for the proper location, size and geometry of spray strips to deflect the whisker spray away from the hull bottom.
- The aerodynamic drag of the hull cross-sectional area above the waterline is also quantified and included in the final performance prediction method.
- Further, the equilibrium trim angle identified in the prediction program (for prismatic hull forms) is, for non-prismatic hulls, related to the trim angle of the $\frac{1}{4}$ buttock line (relative to the level water surface) when measured at the forward edge of the mean wetted length.

INTRODUCTION

The so-called Savitsky Method for predicting the performance of planing hulls was originally published in SNAME's Marine Technology, Volume 1, Number 1, dated October 1964. (Ref.1). This method continues to be used by naval architects even to this date. Briefly, the method combines the elemental hydrodynamic characteristics of prismatic planing surfaces (lift, drag, wetted area, and center of pressure) to determine the equilibrium running conditions (trim, draft, wetted keel and chine lengths, and resistance) and porpoising tendencies of the hull as a function of hull dimensions, loading, deadrise angle, LCG position and speed. The hydrodynamic equations are applicable only to the bottom pressure area aft of the leading edge stagnation line. The wetted bottom area forward of the stagnation line is called the "whisker spray" area. While it is identified in Ref.1, its contribution to the total resistance was not developed at that time. However, as the maximum speeds of planing craft continue to increase, it has been found that the whisker spray contribution to total resistance cannot be ignored.

In 1964, Clement (Ref. 2 & 3) conducted a series of model tests to illustrate the effect of installing spray strips on the bottom of a planing hull in order to deflect areas of the whisker spray away from the bottom. He found that by the use of judiciously located spray strips, (using the results of Ref.1 as a guide), the high speed resistance was reduced by nearly 15%. These results clearly demonstrated the important contribution of whisker spray to total drag. It appears however that no attempt was made to analytically define the whisker spray drag in terms of hull geometry and operating conditions. The present paper identifies the whisker spray (its area, flow direction and location), quantifies its contribution to total drag as a function of trim angle, deadrise angle and speed and incorporates these results into a final prediction procedure. Further, the designer is given guidance as to the location, size, and geometry of spray strips which will deflect the whisker spray away from the bottom.

Since the performance predictive method must include the aerodynamic resistance of the hull cross sectional area above the waterline, this report identifies a typical value of aerodynamic drag coefficient based on model test conducted at the Davidson Laboratory.

Further, an attempt is made to relate the equilibrium running trim angle obtained from Ref.1 (for prismatic hulls) to the 1/4 buttock line profile for non-prismatic hulls.

SYMBOLS

| | |
|-------------|---|
| A_p | bottom pressure area, ft^2 |
| A_s | area of whisker spray in plane perpendicular to keel, ft^2 |
| A_{as} | area of whisker spray in plane of bottom, ft^2 |
| b | beam of planing hull, ft |
| bsr | width of spray deflector, ft |
| C | length of stagnation line, ft |
| C_f | viscous friction coefficient |
| F_s | total viscous force in whisker spray area, lb |
| F_∇ | volume Froude number, $V/\sqrt{g\nabla^{1/3}}$ |
| g | acceleration due to gravity, ft/sec^2 |
| L | length in general, ft |
| L_c | wetted chine length, ft |
| L_k | wetted keel length, ft |
| L_m | mean wetted length of pressure area, $(L_k + L_c)/2$, ft |
| L_{ws} | characteristic length of whisker spray, ft |
| R_s | component of whisker spray resistance in plane of level water surface, lb |
| RN | Reynolds number, VL/ν |
| RN_{crit} | Reynolds number at point of transition of boundary layer flow from laminar to turbulent condition |
| RN_{ws} | Reynolds number of whisker spray, VL_{ws}/ν |
| V | horizontal velocity, ft/sec |
| w | specific weight of water, lb / ft^3 |
| α | angle between keel and stagnation line in horizontal plane, deg |
| β | deadrise angle, deg |

| | |
|-----------------|---|
| δ | bottom angle of spray deflector, deg |
| λ | mean wetted length/beam ratio of pressure area = $(L_k + L_c) / 2b$ |
| θ | angle between forward edge of whisker spray and keel line, deg |
| ν | kinematic viscosity, ft^2 / sec |
| τ | trim angle, deg |
| ξ | break-off angle of spray deflector, deg |
| Δ | vertical load on water, lb |
| $\Delta\lambda$ | increase in non-dimensional wetted length-beam ratio due to whisker spray |
| ∇ | volume, Δ / w , ft^3 |
| Θ | $\theta / \cos \beta$, deg |

DEFINITION OF “WHISKER-SPRAY” AND ITS CHARACTERISTICS

Figure 1 is a sketch, (taken from Ref.1) of the wetted bottom area of the hull when planing. It is seen that the area is actually divided into two regions. One is aft of the stagnation line which is referred to as the pressure area. It is bounded by the wetted keel length ‘Lk’, the wetted chine length ‘Lc’, the transom, and the stagnation line. This is sometimes referred to as the spray root line since the longitudinal distance between these two lines is quite small --especially at trim angles representative of planing hull operation. This is the area that is seen in underwater photographs of the planing bottom (Fig. 2). The direction of the fluid velocity in this area is mainly aft as shown by the orientation of the small woolen tufts which are attached to the bottom. This figure also shows that the flow velocity along the spray-root line is primarily along the direction of the stagnation line. The total viscous drag of the hull is presently computed using only the area aft of the spray root line as the total wetted area.

The other wetted bottom region is forward of the stagnation line and is referred to as the whisker spray area. (see surface E in Fig.3). This area cannot be seen in underwater photographs of a non-transparent hull but can be determined by other means which will be subsequently discussed. At this time, the viscous drag in this area has not been defined so is not included in any analytical methods for computing the total resistance of the hull.

The direction of the fluid flow in this spray area is such that the space angle, δ , between the oncoming free-stream velocity and the stagnation line is equal to the space angle between the direction of the spray velocity and the stagnation line; i.e., any line of motion in the spray area is nearly a reflection about the stagnation line of the incident free-stream velocity. This phenomenon is clearly demonstrated in Fig. 6, taken from Ref. 5, which shows striations in the surface layer of soluble paint applied over the bottom area just forward of the stagnation line (i.e. the striations indicate the direction of the velocity in the spray area). By laying a protractor on this photograph the equality of the incidence angle and the reflected angle is easily seen.

Since the pressure in the spray area is nearly atmospheric, then using Bernoulli’s theorem, the spray velocity can be taken to be equal to the planing speed. Fig.3 is an over-water photograph which shows clearly the extent of the whisker spray as it flows across the bottom. Its reflection on the undisturbed water surface is useful in defining the forward edge of the spray.

As this spray sheet departs from the chine line it resembles a cat’s whiskers—hence the name “whisker-spray”. In model scale, the spray appears as a continuous sheet, while in full-scale, the sheet is broken up into numerous droplets. This is due to the fact that, at small scale, surface tension forces are relatively large compared to the inertia force in the spray and hence tends to maintain the spray in a continuous sheet. In full-scale, the inertia force is substantially greater than the surface tension force and hence the spray sheet will break-up into droplets. In non-dimensional terms the Weber Number (ratio of inertia force to surface tension force) is substantially larger for the full-scale craft. In previous unpublished studies, the Davidson Laboratory added a detergent to the tank water to reduce its surface tension. The spray sheet then broke up into droplets and had the appearance of the full-scale spray. The addition of the detergent had a negligible effect on other measured test results. In the present study, it is assumed that surface tension does not affect the viscous friction drag as the spray flows across the bottom of the hull.

The flow of the spray across the bottom develops a viscous force which has an aft component that adds to the resistance of the hull. It has a negligible effect on the lift force (Ref.3). The objective of the present study is to identify the extent of the whisker spray area over the bottom; estimate its total viscous force; and determine its contribution to the total hull resistance.

Wetted Bottom Pressure Area: The lower half of Fig.1 is a sketch of a planing bottom as seen on a plane that is located along the keel and is perpendicular to the hull centerline. Shown on this sketch are:

Wetted keel length = L_k

Wetted chine length = L_c

Beam = b

Stagnation line

Bottom pressure area A_p = area bounded by L_k , L_c , stagnation line, and transom

$$A_p = \frac{(L_k + L_c) \times b}{2} : \text{(two sides)}$$

Angle between stagnation line and keel = α

Edge of “whisker-spray”

Angle between the keel and the spray edge = θ

Whisker spray area = A_s = area bounded by spray root line, spray edge, and chine.

Also:

Deadrise angle = β

Equilibrium trim angle = τ

Each of these quantities is obtained as follows:

L_k & L_c: For a given loading, deadrise, hull dimensions, and speed, application of the performance computational method for planing hulls given in Ref. 1 will provide the equilibrium values of L_k , L_c and trim angle, τ .

Angle α : Ref.1 develops the following equation which identifies the angle, α ; in terms of the equilibrium trim angle and deadrise angle:

$$\tan \alpha = \frac{\pi \tan \tau}{2 \tan \beta} \quad (1)$$

Length of stagnation line, C: The geometric quantities on the sketch show that:

$$C = \frac{b/2}{\sin \alpha} \quad (2)$$

Angle of spray edge, θ : Experimentally observed bottom flow patterns show that the angle between the spray velocity and the stagnation line can be taken as equal to the angle of the oncoming free stream velocity relative to the stagnation line. This is somewhat analogous to the principle of “reflection” in classical physics as applied, for instance, to reflection of light rays from a rigid surface. It is thus seen from Fig.1 that the angle θ , between the spray leading edge and the keel, is:

$$\theta = 2\alpha \quad (3)$$

Area of whisker spray, A_s : Because of the principle of reflection, the shape of the wetted spray area is that of an isosceles triangle with base dimension equal to the length of the stagnation line and equal values of the base angles, α . Using the above definitions of the various parameters it can be shown that the total whisker spray area (two sides of the hull) projected on the plane along the keel and perpendicular to the hull centerline is equal to:

$$A_s = \frac{b^2 \pi \tan \tau}{16 \sin^2 \alpha \tan \beta} \quad (4)$$

Using the previous definition of α , it is seen that:

$$\tan \tau = \frac{2}{\pi} \tan \alpha \tan \beta \quad (5)$$

Substituting into the Equation (4)

$$A_s = \frac{b^2}{4 \sin 2\alpha} \quad (6)$$

The actual wetted area in the plane of the bottom surface of the hull is:

$$A_{as} = \frac{A_s}{\cos \beta}$$

Thus:

$$A_{as} = \frac{b^2}{4 \sin 2\alpha \cos \beta} \quad (7)$$

This rather simplistic expression for spray area is somewhat different from the complicated equation given in Ref.1. In that reference the spray area is taken as that projected on a plane along the keel and perpendicular to the hull centerline. In the present development the spray area is defined in the plane of the bottom (which is realistic). Further, in Ref. 1, the oncoming fluid, which creates the whisker spray, is indeed reflected from the stagnation line. In contrast, the present report uses the spray-root line as a reference for the reflected flow. The justification for using the spray root line as the reference is that it is located only slightly ahead of the stagnation line; will have a small effect on the magnitude of the spray area; and is readily identified in underwater photographs. The relative simplicity of the proposed formulation, and its acceptable accuracy, justifies its use in this study.

This equation requires some interpretation since it shows that the spray area becomes infinite as β approaches zero degrees. Referring to Equation 1:

$$\tan \alpha = \frac{\pi \tan \tau}{2 \tan \beta}$$

Then, for $\beta = 0$, the stagnation line is at an angle of 90 deg. relative to the keel. Applying the reflection concept discussed above, the spray is then directed entirely in a forward direction so that there is no intersection with the chines. In this case the extent of the spray area is as yet undetermined. Because of its forward velocity, the spray induced viscous forces on a flat bottom, ($\beta = 0$), may actually reduce the hull resistance. This effect was actually noted by Weinstein and Kapryan during high speed tests of a flat planing model conducted in the NACA towing tank in

1953 (Ref. 4). Quoting from paragraph 3 on page 6 of that report “At high trims, the induced drag ($\Delta \tan \tau$) exceeds the total drag and indicates an apparent negative friction force. At these high trims the volume of forward spray is large and appears to have high forward velocity with respect to the model. The relative velocity of the model in the region of forward spray therefore is effectively reversed so that the friction drag due to this spray acts in a direction opposite to that of the drag in the principal wetted area and thereby reduces the total drag”

The present study is however limited to those combinations of trim and deadrise angles which result in the angle of the spray velocity relative to the keel, θ , being equal to or less than 90 degrees. It is obvious that when $\theta = 90$ deg. the spray is directed entirely athwart ship so that there is no longitudinal resistance component due to the viscous force of the spray. The relation between spray induced resistance as a function of trim and deadrise angles is now developed.

Total Viscous Force in Whisker Spray Area

Since the velocity of the whisker spray is taken to be equal to the free stream velocity, V , and the spray area is as defined above, the total viscous force in the spray area, F_s , is:

$$F_s = \frac{1}{2} \rho V^2 A_{as} C_f = \frac{1}{2} \rho V^2 \frac{b^2}{4 \sin 2\alpha \cos \beta} C_f \quad (8)$$

The viscous friction coefficient, C_f , is defined in subsequent sections of this report. The total force, F_s , is in the plane of the bottom and makes an angle $\Theta = \frac{\theta}{\cos \beta}$ relative to the keel (see Fig1).

Contribution of Spray Viscous Force to Total Hydrodynamic Resistance of Planing Hull

The hydrodynamic resistance of a planing hull is defined as the horizontal component of force measured in a plane parallel to the level water surface and in the aft direction. The quantity F_s , defined above, is in the plane of the bottom which has a trim angle and deadrise angle relative to the water surface. This is converted to a resistance component in the plane of the level water surface by the following equation:

$$R_s = F_s \times \cos \Theta \times \cos \tau \quad (9)$$

Since the equilibrium trim angle of typical high-speed planing craft is small (usually less than 6 deg.) the value of $\cos \tau \approx 1.0$ so that this term will be neglected. Thus, R_s can be written as:

$$R_s = \frac{1}{2} \rho V^2 \frac{b^2 \cos \Theta}{4 \sin 2\alpha \cos \beta} C_f \quad (10)$$

It is seen that R_s is very much a function of τ and β which determines the angle Θ . When $\Theta = 90$ deg, the spray direction is perpendicular to the chine, the value of $\cos \Theta = 0$, so that $R_s = 0$ as expected. As the angle Θ decreases (for small values of trim angle and large values of deadrise angle), the equation will show that R_s increases. While this is not immediately obvious from the above equation, recall that the angle α decreases with decreasing trim angle and increasing deadrise angle and appears as $\sin 2\alpha$ in the denominator.

In order to simplify this equation for easy application by the practicing naval architect let:

$$R_s = \Delta\lambda b^2 \frac{1}{2} \rho V^2 C_f = \frac{1}{2} \rho V^2 \frac{b^2 \cos \Theta}{4 \sin 2\alpha \cos \beta} C_f \quad (11)$$

The quantity $\Delta\lambda \times b^2$ represents the increase in effective wetted bottom surface area that is attributed to the whisker spray contribution to total resistance.

Solving for the quantity $\Delta\lambda$:

$$\Delta\lambda = \frac{\cos \Theta}{4 \sin 2\alpha \cos \beta} \quad (12)$$

This expression is plotted on Fig. 4 where the dependence of $\Delta\lambda$ on trim and deadrise is most obvious. It is seen that for combinations of small trim angles and high deadrise angles, that are typical for high speed planing hulls, the added spray resistance will be maximum. Thus, the contribution of the spray viscous force to the total hull resistance can then be written as:

$$R_s = \frac{1}{2} \rho V^2 \Delta\lambda b^2 C_f \quad (13)$$

where

$\Delta\lambda$ is obtained from Fig.4
 b = beam of the planing hull, ft.
 V = planing velocity, ft/sec
 C_f = discussed below

It will be noted from Fig. 4 that, for specific combinations of τ and β the quantity $\Delta\lambda$ is equal to zero. While there will be a noticeable whisker spray breaking away from the chines at these conditions, the direction of its velocity is normal to the keel. Hence there is no longitudinal component of the viscous force and consequently no drag component so that $\Delta\lambda = 0$.

Fig. 5 is a graphical illustration of the effect of trim angle on whisker spray drag for a 15 degree deadrise hull operating at a mean wetted length beam ratio of 1.5. The whisker spray area (shaded area); the total viscous force in the spray area (F_s); and the resistance component (R_s) of F_s are shown for trim angles of 2 deg, 4 deg and 9.5 degrees. It is clear that at the lowest trim angle, 2 degrees, the whisker spray area; F_s ; and its aft orientation, are substantially larger than for the higher trim angles. This results in the largest value of R_s occurring at 2 degree trim. As the trim angle is increased it is seen that these quantities are reduced and that finally, at a trim angle of 9.5 degrees. F_s is directed normal to the keel so that its resistance component is zero. At that point $\Delta\lambda$ is also zero as shown on Fig. 4.

For combinations of small trim angles and high deadrise angles (which are typical for very high speed planing hulls), $\Delta\lambda$ is relatively large so that the spray drag for these hulls will be significant. As will be shown subsequently their whisker spray drag can be as large as 15% of the total drag. Fortunately, short longitudinal spray trips can be judiciously attached to the bottom to deflect the spray and thus avoid the large increase in drag. This report provides guidance as to the proper location, size, and geometry of these spray strips as a function of hull geometry, loading and speed.

Estimate of Friction Coefficient (Cf) in Spray Area

In this study the density and viscosity of the fluid in the whisker spray area are taken to be that of the free stream fluid at the ambient temperature and salinity. Also, since the shape of the spray area is triangular (Fig.1), the characteristic length of the whisker spray (L_{ws}) is taken to be $\frac{1}{2}$ the length of the forward edge of the spray taken in the plane of the bottom. The velocity of the spray sheet is the free stream velocity, V . Thus the Reynolds number of the flow in the spray sheet is:

$$RN_{ws} = \frac{V L_{ws}}{\nu} \quad (14)$$

Using the geometric relations previously identified, the value of L_{ws} is:

$$L_{ws} = \frac{1}{2} \times \frac{b/2}{\sin 2\alpha \cos \beta} \quad (15)$$

Note that L_{ws} will be substantially smaller than the mean wetted length of the pressure area defined as $(L_k + L_c) / 2$. Hence the Reynolds number in the spray area will also be much smaller than that of the pressure area. Further, it has been shown by Savitsky and Breslin (Ref. 6) that the fluid in the spray sheet consists of a thin layer of the oncoming free-surface fluid which is reflected from the stagnation line. It is expected that the level of free turbulence in this layer of fluid is quite small. These observations raise some question as to the state of the model boundary layer in the whisker spray area.

In 1952, Savitsky and Ross (Ref. 5) conducted a series of model tests using a 5 inch beam, 20 deg. deadrise planing hull to determine the state of the boundary layer over a range of Reynolds numbers. A chemical paint detection technique (described in Ref. 5) was used to define the flow patterns over the bottom. The paint was white and was sprayed on the hull bottom which was painted black. Its special characteristic was that it would dissolve from the bottom in turbulent areas--thus exposing the black base color of the model. It would remain white on the bottom where the flow was laminar. In these tests, the model was removed from the towing apparatus after each run and the hull bottom was photographed to record the laminar (white) and turbulent flow (black) areas.

It was found that the flow in the whisker spray area was laminar or in a state of transition from laminar to turbulent flow. Fig. 6 shows that nearly the entire whisker spray area was laminar (white color) for the test condition of 6 deg. trim and a speed of 13.02 ft/sec. Using the above equations, the average Reynolds number of that spray sheet was $RN_{ws} = 1.5 \times 10^5$. This relatively small Reynolds number plus the expected low ambient turbulence level implies an extensive area of laminar flow--thus confirming the experimental observation.

At larger Reynolds numbers it is expected that some portions of the spray area will become turbulent resulting in a combination of laminar and turbulent flow. According to Schlichting, (Ref.7, pg. 538) the boundary layer will be laminar to begin with, and will change to a turbulent one further downstream. The position of the point of transition will depend on the intensity of turbulence in the external flow field and will be defined by the value of the critical Reynolds number, RN_{crit} that ranges between 3×10^5 and 3×10^6 . The viscous drag coefficient, C_f , including the effects of mixed laminar and turbulent flow is identified by Schlichting as:

$$Cf = \frac{0.074}{\sqrt[5]{RN}} - \frac{A}{RN} \quad (16)$$

Where the constant 'A' is related to the Reynolds number at the position of initial transition from laminar to a mixed laminar and turbulent flow. It is called the critical Reynolds number = RN_{crit} . This equation is the Prandtl-Schlichting skin friction formula for a smooth flat plate at zero incidence. (Ref. 7).

The transition point is determined from experimental observations. It is dependent upon the intensity of the turbulence in the external flow. A curve of Cf vs. RN in the transition range (taken from Ref 7) is shown as curve (3a) on Fig. 7 for an assumed transitional $RN_{crit} = 5 \times 10^5$. In this case $A = 1700$. It is seen that, as RN exceeds RN_{crit} , Cf initially increases from its laminar flow value of 0.00188, attains a maximum value, and then decreases for further increases in RN and follows the fully turbulent friction curve at large RN.

In the present study the value of A was estimated by using data from Ref. 2 and 3 where the resistance of the whisker spray was inferred by comparing model test data with and without spray deflectors installed on the hull bottom. Converting the whisker spray drag to a friction coefficient, and knowing its Reynolds number, allowed for a determination of the value of A in Equation 16. The value of A was found to be approximately 4800. This corresponds to a whisker spray $RN_{crit} = 1.5 \times 10^6$ that is well within the range of critical Reynolds numbers specified by Schlichting.

For $RN_{ws} < 1.5 \times 10^6$, the flow is assumed to be laminar and the viscous friction coefficient is taken to be the Blasius formulation (Ref. 7).

$$Cf(\text{laminar}) = \frac{1.328}{\sqrt{RN_{ws}}} \quad (17)$$

The importance of this discussion of the transition of the boundary layer from laminar to turbulent flow pertains mainly to model test results where, for commonly used model sizes, the RN_{ws} will be small enough so that the whisker spray boundary layer will either be fully laminar or in some transitional state between a fully laminar and a fully turbulent state. It may be noted that artificial means for stimulation of turbulence in planing hull model tests are rarely used.

The full-scale craft will operate at much higher RN_{ws} where it is expected that the whisker spray boundary layer will be fully turbulent. In this case, the turbulent friction coefficients such as defined by the Schoenherr friction line (also referred to as the ATTC line) may be used (Ref.8). In summary, the following formulations for estimating the viscous friction coefficient of the whisker spray measured in model tests of Ref. 2 and 3 are expected to apply:

For $RN_{ws} < 1.5 \times 10^6$ (laminar flow):

$$Cf = \frac{1.328}{\sqrt{RN_{ws}}} \quad (18)$$

For $RN_{ws} \geq 1.5 \times 10^6$ (transitional flow):

$$C_f = \frac{0.074}{\sqrt[5]{RN_{ws}}} - \frac{4800}{RN_{ws}} \quad (19)$$

This equation is plotted on Figure 7, curve (5). As expected, because of the larger value of RN_{crit} the values of C_f are less than those given by the transition curve (3a), and the transition to fully turbulent flow occurs at relatively larger RN . This implies a more stable boundary layer in the model bottom area wetted by the fluid that comprises the whisker spray. Because this equation is based on a limited amount of available model data, there is still some concern about its applicability to the relatively thin layer of fluid that flows along the hull bottom. Further analytical and experimental studies of the viscous characteristics of this relatively thin layer of flow are strongly recommended.--of particular usefulness would be experiments that directly measure the whisker spray drag and relate these results to model size. Of course full scale tests would be invaluable.

In conclusion, transitional flow equations such as in Eq. 18 and 19, should be applied to model test results where the boundary layer is expected to be in a laminar or transitional state and the Schoenherr or ITTC lines be used for full-scale estimates where the boundary layer is expected to be fully turbulent. Because the value of A in Eq. 16, is governed by the environmental conditions in a test facility, the transitional flow equation may be different in different towing tanks.

VALIDATION OF WHISKER SPRAY DRAG EQUATION

Wherever possible, the results of analytical predictions should be verified by comparison with experimental results. Unfortunately, there are no direct measurements of the whisker spray drag in the published literature. However there are three sources of model test data that can be used indirectly to obtain estimates of spray drag that can be compared with the recommended equation for spray drag. These are:

- 1) A series of model test results that demonstrated the effectiveness of judiciously located bottom spray strips in reducing the total resistance of high-speed planing hulls. (Ref. 2 and 3). The whisker spray drag was inferred from the test data and then compared with the computed drag.
- 2) A series of high speed model tests performed by Kapryan and Weinstein (Ref. 9) on a 20 degree deadrise prismatic hull over a wide range of trim angles and wetted lengths. By comparing the total model friction drag coefficient with the Schoenherr turbulent friction line, it was possible to identify the whisker spray drag.
- 3) Model test results of a number of randomly selected planing hulls where the measured total resistance is compared with the computed total resistance that includes hull resistance + whisker spray resistance + aerodynamic resistance. These results provide for a validation of the performance prediction method as originally presented in Ref 1. *but* now expanded to include the spray and aerodynamic contributions to resistance.

Prior to discussing these model tests it is important to note that, in most test reports the model data have been extrapolated to and are presented as full-scale values. This raises the question as to how the model whisker spray resistance has been extrapolated to the larger Reynolds numbers of the full-scale craft. The answer is that, at the present time, no separate extrapolation is made of the whisker spray resistance to account for their Reynolds numbers in the full-scale craft. The

current procedure is to use only the wetted bottom area aft of the stagnation line in calculating the model viscous resistance and then subtract this from the total measured resistance (which is the sum of induced pressure drag + viscous drag in the bottom area aft of the spray root line + the whisker spray drag + aerodynamic drag) to obtain the residual drag. The part of the bottom area that is wetted by the whisker spray is customarily neglected (Ref 10). Consequently, the model viscous spray drag component is, by default, contained in the calculated model residual drag.

Since the full-scale residual drag is taken to be equal to the model residual drag multiplied by the cube of the scale ratio it consequently scales the model whisker spray drag by the cube of the scale ratio. This implies that the friction coefficient in the spray area is the same for the model and full-scale which of course is not correct. The published data are nevertheless quite useful since they can be used to isolate the resistance of the model whisker spray drag, for which the Reynolds number are known, and then to compare these experimental results with analytical predictions using the C_f vs. RN relations given by Equation 18 and 19. This procedure is applied in the following sections of this report.

Each of the above validation efforts is discussed in the following sections.

1) Model Tests With and Without Spray Deflectors

In 1964, Clement (Ref. 2 & 3), conducted model tests on two planing hulls to examine the effectiveness of adding bottom spray strips to deflect the whisker spray away from the hull and, thus reduce the total hydrodynamic resistance. Each model was tested with and without spray strips and the results presented as full-scale values. The difference in measured total resistance was used to identify the effectiveness of these strips and also, indirectly, to quantify the magnitude of the resistance of the whisker spray to the extent that it was deflected from the bottom.

A brief description is given of the model geometries; model scale; loading; size and location of spray strips; test results; and comparison between calculated and measured value of the whisker spray drag.

Results from Reference 2: The model used for these tests represented a 68-ft planing boat to a scale of 1/6. The model resistance data was converted to a full-scale displacement of 99,500 lb using the Schoenherr coefficients of frictional resistance (also called the ATTC friction line) with zero roughness allowance. The body plan for this hull and the arrangement of the short spray deflector strips are shown on Fig 8. The deadrise angle is 20.5 deg. and the equivalent full-scale beam, measured between the chines is 15.6 ft. (model beam = 2.6 ft.). The bare hull (no bottom spray strips) performance results for this hull are given by the solid curves shown in Fig. 9. All results are presented in non-dimensional form.

Longitudinal spray strips were then attached to the hull bottom as shown in Fig 8. As can be seen, they were relatively short, and extended from just aft of the spray root line forward into the whisker spray area. Each strip deflects a portion of the whisker spray from the bottom and produces a local dry bottom area that extends from the outboard edge of the spray strip to the chine. By judiciously locating a number of such small spray strips (in a chevron like pattern) as shown in Fig. 8, it is possible to deflect a substantial area of the whisker spray away from the bottom. The results of model tests with these spray strips are shown by the round symbols on Fig

9. It is clear, that the addition of spray strips reduced the high-speed resistance by 6% without an increase in low speed resistance or change in trim, and heave.

The difference between the resistance of the bare hull and the hull with spray strips can be taken to be indicative of the whisker spray resistance. Since the plotted data also defines the running trim angle vs. speed, the spray drag was calculated for each speed using Equation 13 of this report. The details of this calculation and results are tabulated below:

$$R_s = \frac{1}{2} \rho V^2 \Delta \lambda b^2 C_f$$

where:

$$\Delta \lambda = f(\tau, \beta) \text{ given on Fig. 4}$$

$$b = \text{beam of the planing hull model} = 2.6 \text{ ft.}$$

$$V = \text{model planing velocity, ft/sec}$$

$$C_f = \frac{0.074}{\sqrt[5]{RN_{ws}}} - \frac{4800}{RN_{ws}} \text{ (for transitional flow, } RN_{ws} \geq 1.5 \times 10^6 \text{)}$$

$$C_f = \frac{1.328}{\sqrt{RN_{ws}}} \text{ (for laminar flow, } RN_{ws} < 1.5 \times 10^6 \text{)}$$

$$RN_{ws}(\text{model}) = \frac{V Lws}{\nu}$$

$$Lws = \frac{1}{2} \times \frac{b/2}{\sin 2\alpha \cos \beta}$$

The spray area used in this equation is the total wetted spray area as given by Equation 7. However, Fig. 8 shows that the spray strips deflected only approximately 88% of the total spray area so that the R_s was taken to be 88% of the calculated value based on total spray area. Thus, for the deadrise angle of 20.5 deg., and a displacement of $\Delta=99,500$ lbs:

| $\frac{F_V}{\Delta}$ | τ | $\frac{\Delta \lambda}{\Delta}$ | 2α | Lws^{**} | RN^{**} | C_f^{**} | R_s^* | $\frac{R_s}{\Delta^*}$ |
|----------------------|---------|---------------------------------|-----------|------------|-------------------|------------|---------|------------------------|
| 2.8 | 4.7 deg | 0.33 | 38.0 deg | 2.13 ft | 3.7×10^6 | 0.0023 | 410 lbs | 0.0047 |
| 3.2 | 4.5 | 0.35 | 36.6 | 2.21 | 4.4×10^6 | 0.0024 | 680 | 0.0068 |
| 3.6 | 4.2 | 0.39 | 34.2 | 2.36 | 5.2×10^6 | 0.0024 | 940 | 0.0094 |
| 3.8 | 4.0 | 0.40 | 32.8 | 2.45 | 5.7×10^6 | 0.0024 | 1100 | 0.0111 |

* = Full scale values

** = Model values

These calculated values of spray drag/displacement ratio were then subtracted from the bare hull drag/displacement ratios on Fig. 9 to obtain the hull resistance/displacement ratio when spray strips are added to the bottom. The results are plotted on Fig. 9 and show rather good agreement with the experimental results, thus providing some credibility to the proposed analytical method for estimating the drag of the whisker spray.

Results from Reference 3: Of course the conclusions from a single test may be fortuitous. Fortunately, Clement conducted similar tests on a 1/10 scale model of hull No. 4666 of the Series 62 family of hard chine planing hulls (Ref. 3). Body plans and the arrangement of the spray deflector strips are shown on Fig 10. There were short length strips similar to those used in the tests of Ref.2 and long strips whose aft end was just aft of the spray root line and whose forward

end extended to the chine. The deadrise angle is 12.5 deg, and the equivalent full-scale beam measured between the chines at mid-ship is 18.7 ft. (model beam = 1.87 ft.). The test results, which were extrapolated to a weight of $\Delta = 101,800$ lbs, are shown on Fig 11 for the hull with and without spray strips. Experiments were conducted at a considerably higher speed than the model tests of Ref 2. Two lengths of spray strips were used in these tests. Using the procedure demonstrated above, and again assuming that 88% of the calculated maximum spray area was wetted, the following values of whisker spray drag are calculated.

| F_V | τ | $\Delta\lambda$ | 2α | Lws^{**} | RN^{**} | C_f^{**} | R_s^* | R_s/Δ^* |
|-------|---------|-----------------|-----------|------------|-------------------|------------|---------|----------------|
| 4.5 | 2.9 deg | 0.31 | 39.4 deg | 0.76 ft | 1.6×10^6 | 0.0013 | 940 lbs | 0.010 |
| 5.0 | 2.6 | 0.35 | 35.6 | 0.82 | 1.9×10^6 | 0.0016 | 1630 | 0.015 |
| 5.5 | 2.2 | 0.43 | 30.4 | 0.95 | 2.5×10^6 | 0.0019 | 2860 | 0.028 |
| 6.0 | 2.0 | 0.48 | 27.8 | 1.03 | 3.0×10^6 | 0.0021 | 4190 | 0.041 |

* = Full scale values

** = Model values

These calculated values of spray drag/displacement ratios were then subtracted from the bare hull drag /displacement ratios on Fig. 11 to obtain the hull resistance/displacement ratio when spray strips are added to the bottom. The results are also plotted on Fig. 11 and again show rather good agreement with the experimental results. It should be noted that, at the highest speed, $F_V = 6.0$, the whisker spray drag was approximately 18% of the total drag—clearly a significant addition to the hull total drag. (note the low trim at the highest speed which results in large values of $\Delta\lambda$).

2) Model Tests of a 20 deg. Deadrise Prismatic Hull (Ref. 9)

In 1953, Kapryan and Boyd (Ref. 9) published the results of an extensive series of model tests of a 20 deg deadrise, 4.125 in. beam, prismatic planing surface with vertical chine strips that resulted in an effective deadrise of 16 deg (Fig. 12). In these tests measurements were made of the resistance, wetted length, center of pressure, and draft for a range of fixed trim angles and high speeds. All tests were conducted behind a wind screen so that aerodynamic forces on the model were very small. Of particular interest to the present study was their analysis of the model resistance data. The authors calculate the friction drag coefficient by subtracting the induced drag coefficient, $(\Delta \tan \tau) / (1/2)\rho V^2 Lm b$, from the total measured drag coefficient. Since the aerodynamic forces on the model were negligible, this procedure provides the total viscous drag coefficient that includes the viscous forces on the bottom pressure area and the whisker spray area but normalized by only the bottom pressure area. The results are plotted against hull Reynolds number on their Figure 15 for the 20 deg. deadrise hull along with the Schoenherr (ATTC) turbulent friction line. This plot is reproduced in the present report as Figure 13. Although the drag data are somewhat scattered, the following trends can nevertheless be observed.

Of particular interest is that the calculated friction coefficients generally lie above the Schoenherr line even though the model surfaces were “extremely smooth”. Further, this difference is largest at the 2 deg trim angle and decreases with increasing trim angle until, at a trim angle of 12 degrees the differences are negligible. Kapryan and Boyd note these differences and, in paragraph 4 on their Pg. 5, state that “this result is apparently associated with the method of calculation and requires further investigation for a more accurate estimation of large-scale resistance”

The present authors suggest that the larger than expected calculated friction coefficients are a result of the neglect of the whisker spray wetted area in normalizing the total viscous force—only the bottom pressure area was used. Recall that the total viscous force given in Ref.9 must be the sum of the viscous forces in both the bottom pressure and whisker spray areas. Using this smaller area for normalizing the total friction drag will of course result in larger friction coefficients.

The fact that the differences between the calculated and Schoenherr friction coefficients increase with decreasing trim angle is consistent with the whisker spray drag characteristics as developed in the present report. As shown in Fig.4, the value of $\Delta\lambda$, which quantifies the whisker spray drag, is largest for the lowest trim angle, and for a deadrise angle of 16 deg. is essentially zero at 12 deg. trim. These trends are consistent with the experimental results plotted on Fig. 13.

To quantify these conclusions the whisker spray drag was calculated for combinations of 16 deg. deadrise and trim angles of 2, 4, 6 and 12 deg. using the methods previously developed and illustrated in the present report. In these calculations it was found that the original Prandtl-Schlichting formula, (where $A = 1700$ in equation 16), for the friction coefficient in transitional flow was more suitable than the formulation used to represent the data obtained in model tests conducted at the Davidson Laboratory and the David Taylor Model Basin. These results were added to the viscous drag in the pressure area and the total normalized by the pressure area. The results are plotted on Fig. 13. It is seen that the inclusion of the whisker spray drag provides results that more nearly agree with the mean of the scattered experimental data.

Thus, it is concluded that the results of Ref. 9 provide further credibility to the existence of whisker spray and to the method for estimating its magnitude as developed in this paper.

3) Model Tests of Randomly Selected Planing Hulls

Computational Procedure: Having developed methods for estimating the whisker spray drag and the aerodynamic drag, (see Appendix 1) these will now be combined with the bare hull performance prediction method of Ref.1 to provide a complete analytical method for predicting the total drag of an unappended (no struts, shafts, rudders, cooling water intake scoops, superstructure, etc.) planing hull. The data from several randomly selected planing hull designs, that were model tested at the Davidson Laboratory, are used to compare with the analytical results. It is important to remember that the model to full scale extrapolation procedures used by towing tank facilities do not separately account for the Reynolds number of the whisker spray. Instead, by default, its drag becomes one component of the residual drag of the model (see previous discussion).

The procedure is as follows:

- 1) For a given test model, its scale; deadrise angle, and beam (measured between the chines) at the LCG; the frontal area of the hull cross-section as measured above the keel; the LCG (measured from the transom); corresponding displacement; and the thrust shaft angle relative to the level water surface are identified.
- 2) These parameters become inputs to the bare hull performance prediction method given in Ref.1. The program is rapidly exercised on a desk-top computer for a range of speeds. The

outputs are given in full-scale values of hull drag; wetted keel and chine lengths; draft; and equilibrium trim angle as a function of speed.

It is essential to understand that the method of Ref. 1 is limited to those operating conditions where the computed wetted keel length does not extend into the upturned bow area. This condition introduces an additional bow drag component which is not accounted for in the computational method. Of course a well designed planing hull will avoid wetting of the bow region when planing at high speed. The computations are thus limited to speeds where L_k is less than approximately equal to 0.90 LWL.

- 3) The computed values of trim angle are then used to calculate the drag of the whisker-spray using the procedure demonstrated in previous sections of this report. Recall that the model whisker spray friction coefficient must be used for comparison with published full scale predictions.
- 4) Using the frontal area of the bare hull and a nominal drag coefficient (based on frontal area) = 0.70, (see Appendix 1), the aerodynamic drag of the model is easily calculated as a function of towing speed. This is multiplied by the cube of the model scale ratio to obtain the full-scale aerodynamic drag for zero ambient wind speed. In the total design it is of course necessary to include the drag of appendages, superstructure, etc. for a complete resistance estimate.
- 5) Finally, the addition of items (2), (3), and (4) provides a computed estimate of the total drag of an unappended hull as function of speed. The results are compared with model test results (extrapolated to full scale values) to judge the validity of the proposed computational method and to demonstrate the potentially significant contributions of whisker spray and aerodynamic resistance to the total resistance of a planing hull at high speed.

Model Test Results: Four hard chine planing hulls that were model tested at the Davidson Laboratory, Stevens Institute of Technology were randomly selected to be used in this study. They varied in deadrise angle, length, beam, displacement, LCG and test speed range. The model data were extrapolated to full scale values using standard towing tank procedures (as discussed previously) and the Schoenherr turbulent friction coefficient line. Some hulls used a roughness allowance of 0.0004 while others used zero roughness allowance.

These results are presented in Tables 1 - 4. Each table contains a body plan of the specific hull; the principal full scale geometric dimensions; test displacement; LCG; shaft angle; roughness allowance; frontal area of the hull above the keel; dimensions of skeg (if one was used); and the scale of the test model. The full scale total resistance vs. full scale speed is plotted on the lower part of each table.

Computational Results: Tables 1 – 4 also contain the calculated values of full-scale resistance vs. speed. For each hull the following calculated components of resistance are tabulated separately:

- 1) Bare hull resistance vs. speed
- 2) Aerodynamic resistance vs. speed
- 3) Whisker spray resistance vs. speed
- 4) Total resistance vs. speed.

The methods for calculating each of these resistance components are defined in the Tables.

Items 1 and 4 are plotted on the lower part of each Table for comparison with the model test results. Of particular interest, these plots also define the speed below which the calculated wetted keel length is estimated to be less than approximately equal to 0.90 LWL thus precluding the use of the computational method for bare hull resistance for this speed range.

Comparison of Computed vs. Experimental Results: It is seen that, for all test hulls, the differences between calculated total resistance and the results from model tests are less than 5 %. This is indeed encouraging since the calculated total resistance is comprised of the sum of three separately computed components.

Further, as previously shown, the agreement between the calculated whisker spray resistance and that measured directly by Clement (Ref. 2 and 3), and the test results of Ref. 9 provide additional credibility to the analytical method proposed in this report.

To the authors' knowledge the present effort appears to be the first study to analytically quantify the effect of whisker spray on the total resistance of a planing hull. Hopefully it will encourage additional research particularly as regards the viscous friction coefficient of the thin sheet of water that constitutes the whisker spray. It has been assumed that, in model tests, there is a mixture of laminar and turbulent flow in the spray boundary layer and a transitional friction coefficient is required to quantify the friction coefficient as a function of whisker spray Reynolds number. It is believed that further experimental and analytical studies are necessary to understand this flow regime and to develop appropriate viscous coefficients that will be applicable for both model and full-scale Reynolds numbers.

Discussion of Results: The data in Tables 1-4 illustrate the relative importance of the contribution of whisker spray to the total resistance of a high speed planing hull. Using the hull shown on Table 2 as an example, the following observations are summarized:

1. The whisker spray resistance increased approximately as the 4.3 power of the speed and was nearly 12% of the bare hull resistance at a maximum speed of 46 knots. This is due mainly to the fact that the trim angle decreases from 9.2 deg at 20 knots to 3.53 deg at 46 knots. Based on the earlier discussions, the lower trim angle orients the spray velocity to a more aft direction so the longitudinal component of its resultant viscous force is increased- thus increasing the hull resistance. The quantity, $\Delta\lambda$, which is a direct indicator of the importance of spray resistance, is seen to increase from a value of 0.06 at 20 kts to a value of 0.42 at 46 knots. This results in a seven fold increase in resistance due just to a decrease in trim angle. When the quadratic effect of speed is included the spray drag at 46 kts will be 37 times greater than at 20 kts.

Since high speed planing hulls are expected to have high deadrise and will naturally run at relatively low trim angles, Figure 4 shows that the quantity $\Delta\lambda$ will attain large values and hence these hulls are expected to have large spray induced resistance components. Thus, it is imperative that these hulls be fitted with spray deflectors mounted on the bottom. Recommendations for proper location and design of these deflectors are discussed further in the following section of this paper.

2. The aerodynamic resistance at 46 kts is nearly 6% of the tabulated bare hull resistance. When combined with the whisker spray resistance their sum will increase the bare hull resistance by nearly 18%. Hence when using the computational method of Ref. 1 it is essential that, at high speed, the whisker spray and aerodynamic resistances be added to the results of that computation.

3. The computational method of this paper will allow similar evaluations to be made for other hulls given their geometry, loading, and speed. In some cases it may be that, while there is visual evidence of whisker spray emanating from the chines, the combination of running trim and hull deadrise will be such as to direct the spray perpendicular to the keel so that $\Delta\lambda = 0$ and there is no spray contribution to hull resistance.

SUMMARY

These studies indicate that the suggested approach to estimating the whisker-spray resistance appears to be viable. While there is reasonable agreement between the calculated and inferred values of spray resistance (based upon three separate series of model tests) the suggested values of model viscous drag coefficient, C_f , in the transition area of the whisker spray must still be verified. It is recommended that additional studies, both experimental and analytical, be made to further quantify C_f in the whisker spray area.

LOCATION AND DESIGN OF WHISKER SPRAY DEFLECTORS

Location and Area of Whisker Spray

The boundaries of the whisker spray flow along the bottom are readily defined by applying the results of calculations such as presented in Tables 1-4. Specifically, again using the hull in Table 2 as an example, the following procedure is suggested:

- 1) The bare hull resistance calculations (item 1) provide the running wetted keel length, L_k , and wetted chine length, L_c , as a function of speed—the line connecting L_k and L_c along the bottom defines the aft boundary of the whisker spray and makes an angle, α , with the keel measured in a plane perpendicular to the hull longitudinal centerline. This is illustrated on Fig.1.
- 2) The whisker spray resistance calculations (item 3) define the angle $\theta = 2\alpha$. This is the angle between the forward edge of the spray and the keel, measured in a plane perpendicular to the hull longitudinal centerline. This is also illustrated on Fig.1.
- 3) The bottom area wetted by the whisker spray is thus that bounded by the forward and aft edges of the spray and the chines as shown by the shaded area on Fig.1.

Placement and Size of Spray Deflectors

Clement (Ref. 2, 3), demonstrated that, three relatively short, longitudinally staggered deflectors whose aft ends are just aft of the stagnation line and are mounted normal to each side of the bottom will effectively deflect approximately 88 % of the spray away from the bottom. As shown in Fig.8, the transverse locations of the spray strips are approximately $\frac{1}{4}$, $\frac{1}{2}$, and $\frac{3}{4}$ of the half beam outboard of the keel. The longitudinal location is such that the aft ends of each strip extend somewhat aft of the stagnation line at each transverse location of the strips. Since the spray location and orientation are functions of speed and loading, the designer should decide the most favorable location of the deflectors to accommodate the high- speed range of operation.

Calculated results such as given in Tables 1-4 will provide the necessary guidance for locating and sizing the spray deflectors.

The results of Clement's and the present study clearly demonstrate that spray deflectors should be relatively short. If they are so long that they extend into the pressure area where the fluid flow is essentially in a longitudinal direction, this extra length will have no effect on the spray but will only add to the total resistance of the hull.

Cross Section Shape of Spray Deflectors

Muller-Graf (Ref.11) presents the results of an extensive series of model tests to develop a so-called "advanced spray rail system" for semi-displacement hulls. Of particular interest to the planing hull community is the suggested triangular cross-sectional shape of the deflector as shown in Fig.14. The sharp outer edge is necessary to facilitate the separation of spray from the hull. Other features are:

$$\begin{aligned}\zeta &= \text{break-off angle of spray deflector } >90 \text{ deg.} \\ \delta &= \text{bottom angle of spray deflector } \cong 8 \text{ deg.} \\ b_{sr} &= \text{width of spray deflector } \cong 0.005 \text{ LWL}\end{aligned}$$

The recommended sharpness of the outer edge of the deflector cannot be overemphasized. Even a slight rounding of this edge may cause the flow to remain attached to the deflector and thus reduce its ability to deflect the spray sheet. Clement (Ref. 2) shows that a rounded edge (approximately $\frac{1}{4}$ in., full scale) nearly negated the effectiveness of the deflector. This may present a problem for hulls that are constructed in molds where the spray deflectors are an integral part of the bottom and thus may be difficult to manufacture with a sharp outer edge.

RELATION BETWEEN CALCULATED and MEASURED TRIM ANGLE

The computational method of Ref. 1 is based on the hydrodynamics of prismatic surfaces where the buttock lines are straight and parallel. Thus, the calculated trim angle, relative to the level water surface, is the same for every buttock line. This angle is referred to as the "hydrodynamic" trim angle.

The reference for the trim angle recorded by towing tanks during tests of conventional warped (non-prismatic) hulls may vary according to the preferences of the test facility or the designer. For example, the trim angle may be the angle between the keel and the level water line; the angle between the lower edge of the skeg and the level water line; the angle of the design water line relative to the level waterline, etc. Consequently, a direct comparison of the calculated trim with the trim angle reported by the towing tank may not be meaningful.

A brief attempt was made to correlate the computed trim angle with the geometry of the tested non-prismatic hulls. Some of the tested hulls had a small amount of warp (deadrise increasing with increasing distance forward of the transom.) so that the buttock lines were at a positive trim angle relative to the level water surface even in the static condition. Other hulls had a shallow transom draft so that the aft length of the keel was at a negative trim relative to the level water line in the static condition. Consequently, when planing, the angle of attack (relative to the level water surface) at any point on the bottom varies according to its longitudinal and transverse

location. It would be useful to establish both an effective trim and deadrise for warped surfaces. This will require additional systematic model tests supported by analytical studies. Unfortunately, presently there is no apparent sponsor for such a study.

In the interim, the present limited study suggests that the effective deadrise for a warped surface can be taken as that at the LCG. Relative to the effective trim angle, the results of this study suggests that the effective trim can be taken as the geometric trim angle of the 1/4 buttock line measured at the forward edge of the mean water line.

CONCLUSIONS

An analytical procedure is developed for calculating the resistance of the leading edge whisker spray associated with planing craft. It is shown that the magnitude of this resistance component is dependent upon the running trim and hull deadrise. It is largest for high deadrise hulls operating at relatively low trim angles—a combination that is typical for very high-speed hulls. In fact, the whisker spray resistance can be as large as 15% of the bare hull resistance and must be included when estimating the total resistance of high-speed hulls. The present report applies the computation method to estimate the total resistance of four randomly selected planing hulls that were model tested at the Davidson Laboratory and shows rather good agreement with experimental data.

It is shown that the whisker spray can be deflected from the hull bottom (with a consequent reduction in hull resistance) by installing relative short longitudinal spray strips mounted normal to the bottom. Guidance is provided for the proper location, size, and geometric shape of these strips.

In model tests, the whisker spray flow along the bottom is shown to be in a transitional state between laminar and turbulent flows. An equation for its friction coefficient as a function of local Reynolds number is developed. However, it is recommended that further experimental and analytical studies be undertaken to further define the viscous coefficient for model and full-scale planing craft.

ACKNOWLEDGMENT

The authors are indebted to the T&R Steering Committee of The Society of Naval Architects and Marine Engineers for their encouragement to undertake and to provide partial financial support for this study. Perhaps the results of this effort will encourage further research of the whisker spray phenomenon associated with planing hulls.

REFERENCES

1. Savitsky, Daniel: "Hydrodynamic Design of Planing Hulls" SNAME Marine Technology, Vol.1, No 1, October, 1964.
2. Clement, Eugene P. "Effects of Longitudinal Bottom Spray Strips on Planing Boat Resistance" DTMB, Department of the Navy, Report No. 1818, February, 1964
3. Clement, Eugene P. "Reduction of Planing Boat Resistance by Deflection of the Whisker Spray" DTMB, Department of the Navy, Report No 1929, November, 1964.
4. Weinstein, Irving and Kapryan, Walter,J. " The High-Speed Planing Characteristics of a Rectangular Flat Plate Over A wide Range of Trim Angle and Wetted Length" NACA Technical Noe 2981, July, 1953.
5. Savitsky, Daniel and Ross, Edward W. "Turbulence Stimulation in the Boundary Layer of Planing Surfaces-Part II" Davidson Laboratory, Stevens Institute of Technology, Report No. 444, August, 1952.
6. Savitsky, Daniel, and Breslin, John P. "On the Main Spray Generated by Planing Surfaces" Davidson Laboratory, Stevens Institute of Technology Report No. 678, January, 1958.
7. Schlichting, Herman. "Boundary Layer Theory" Fourth Edition, Published by McGraw-Hill Book Company, Inc. 1960
8. SNAME Bulletin No. 1-2 (1948) "Uniform Procedure for the Calculation of Frictional Resistance and the Expansion of Model Data to Full Size" Published by The Society of Naval Architects and Marine Engineers, Jersey City, NJ
9. Kapryan, Walter J. and Boyd., George M. Jr. "The Effect of Vertical Chine Strips on the Planing Characteristics of V-Shaped Prismatic Surfaces Having Angles of Deadrise of 20 deg. and 40 deg. NACA Technical Note 3052. November, 1953.
10. Clement, Eugene P. and Blount, Donald L. "Resistance Tests of a Systematic Series of Planing Hull Forms" SNAME Transactions, Vol. 71, 1963
11. Muller-Graf, Burkhard. "The Effect of an Advanced Spray Rail System on Resistance and Development of Spray of Semi-Displacement Round Bilge Hulls." FAST '91

Appendix 1

AERODYNAMIC RESISTANCE OF PLANING HULL MODELS

The performance prediction method in Ref.1 does not include the aerodynamic drag of the hull cross-sectional area above the waterline. This is of importance during model tests where the design naval architect may be comparing tank data (using a hull model without super-structure) with computer estimates. Because this aerodynamic drag increases as the square of the towing speed, it becomes a significant component of the total resistance at maximum speed.

In order to quantify this drag component, the Davidson Laboratory measured the drag of many models of mono-hull planing hulls towed over a wide speed range with the hulls set at a trim angle of zero degrees and raised just above the level water-line. (There was no hull wetting). It was found that, for typical bow plan-forms, the drag coefficient, based on frontal area of the hull was approximately equal to 0.70.

Thus the aerodynamic drag of the hull can be estimated by the following simple equation.

$$R_{Air} = \frac{1}{2} \rho_{Air} V^2 Ah \times Cd \quad (20)$$

where:

R_{Air} = aerodynamic resistance of hull

V = velocity, (towing speed \pm wind speed), ft/sec

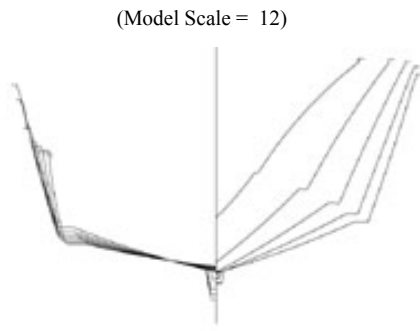
Ah = frontal area of hull, ft²

ρ_{Air} = air density, lb-sec² / ft⁴

Cd = aerodynamic drag coefficient based on frontal area of the hull = 0.70

Of course the naval architect will include both the hull frontal area and the above deck structure when estimating the total aerodynamic resistance of the craft. These resistance components must be included when estimating the powering requirements of planing craft at high speed.

Table 1: Computed v. Measured Total Resistance



(Model Scale = 12)

Geometry and Test Conditions

(Full Scale Values)

- Δ = 115,000 lbs
- LCG = 28.4 ft forward of transom
- Beam @ LCG = 18.2 ft
- Deadrise @ LCG = 14 deg
- Shaft angle = 12 deg
- Frontal area of hull above keel = 216 ft²
- LOA = 81.5 ft
- Roughness allowance = 0.0004
- Skeg @ Keel: L = 36 ft.: Area = 65 ft².: Thickness = 0.40 ft.

1) Bare Hull Resistance (Use method described in Ref 1) + Skeg Resistance

| Vk | V (ft/sec) | τ (deg) | Lk (ft) | Lc (ft) | RBARE HULL+SKEG (lbs) |
|----|------------|--------------|---------|---------|-----------------------|
| 28 | 47.3 | 3.94 | 63.0 | 42.0 | 13060 |
| 34 | 57.4 | 3.84 | 60.9 | 39.9 | 14590 |
| 38 | 64.1 | 3.59 | 58.1 | 36.2 | 15410 |
| 42 | 70.9 | 3.30 | 56.8 | 33.3 | 16310 |
| 44 | 74.3 | 3.16 | 56.4 | 30.8 | 16820 |

2) Aerodynamic Resistance =Ra (Use Equation 20):

| Vk | 28 | 34 | 38 | 42 | 44 |
|--------|-----|-----|-----|-----|-----|
| Ra,lbs | 400 | 580 | 730 | 890 | 980 |

$\rho_{air} = 0.00234$ slugs/ft³

3) Whisker Spray Resistance (Use Equation 13 and associated example)

| Vk | τ | $\frac{\Delta \lambda}{L}$ | 2α | Lws** | RNws** | Cf** | Rws* |
|----|---------|----------------------------|-----------|---------|----------|--------|---------|
| 28 | 3.9 deg | 0.27 | 43.4 deg | 0.57 ft | 7.23E+05 | 0.0016 | 300 lbs |
| 34 | 3.8 | 0.28 | 42.4 | 0.58 | 8.95E+05 | 0.0014 | 410 |
| 38 | 3.6 | 0.30 | 39.9 | 0.61 | 1.05E+06 | 0.0013 | 520 |
| 42 | 3.3 | 0.34 | 36.9 | 0.65 | 1.24E+06 | 0.0012 | 650 |
| 44 | 3.2 | 0.36 | 35.4 | 0.68 | 1.35E+06 | 0.0011 | 720 |

* = full scale; ** = model scale; $v = 0.00001078$ ft²/sec (model tests)

4) Total Resistance Rt = RBAREHULL+SKEG + Ra + Rws

| Vk | 28 | 34 | 38 | 42 | 44 |
|--------|-------|-------|-------|-------|-------|
| Rt,lbs | 13760 | 15580 | 16660 | 17850 | 18520 |

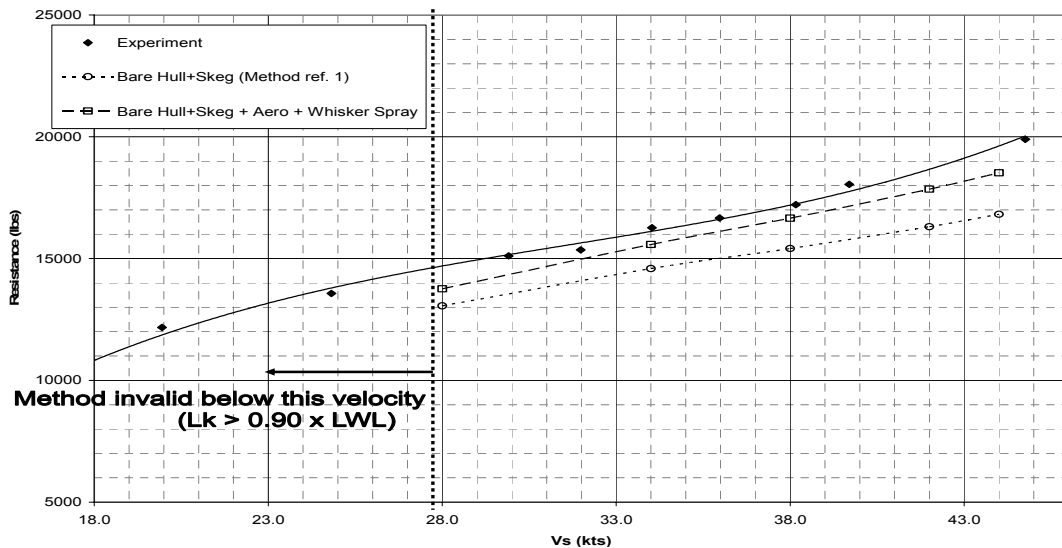
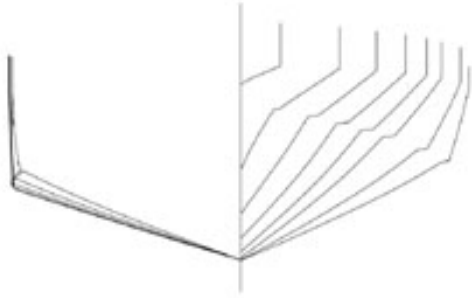


Table 2: Computed v. Experimental Total Resistance

(Model Scale = 8)



Geometry and Test Conditions

(Full Scale Values)

- Δ = 38,750 lbs
- LCG = 13.13 ft forward of transom
- Beam @ LCG = 31.1 ft
- Deadrise @ LCG = 19 deg
- Shaft angle = 0.0 deg
- Frontal area of hull above keel = 65 ft²
- LOA = 41 ft
- Roughness allowance = 0.0004

1) Bare Hull Resistance (Use method described in Ref 1)

| Vk | V (ft/sec) | τ (deg) | Lk (ft) | Lc (ft) | RBARE HULL (lbs) |
|----|------------|--------------|---------|---------|------------------|
| 20 | 33.8 | 9.2 | 25.1 | 16.3 | 6970 |
| 25 | 42.2 | 7.53 | 24.9 | 14.0 | 6270 |
| 30 | 50.6 | 6.12 | 25.5 | 12.1 | 5810 |
| 35 | 59.1 | 5.05 | 26.6 | 10.4 | 5630 |
| 40 | 67.5 | 4.25 | 28.0 | 8.6 | 5710 |
| 46 | 77.6 | 3.53 | 29.8 | 6.5 | 6070 |

2) Aerodynamic Resistance = Ra (Use Equation 20):

| Vk | 20 | 25 | 30 | 35 | 40 | 46 |
|--------|----|----|-----|-----|-----|-----|
| Ra,lbs | 60 | 90 | 140 | 190 | 240 | 320 |

$\rho_{air} = 0.00234$ slugs/ft³

3) Whisker Spray Resistance (Use Equation 13 and associated example)

| Vk | τ | $\Delta\lambda$ | 2α | Lws** | RNws** | Cf** | Rws* |
|----|---------|-----------------|-----------|---------|----------|--------|--------|
| 20 | 9.2 deg | 0.06 | 72.9 deg | 0.45 ft | 5.01E+05 | 0.0019 | 20 lbs |
| 25 | 7.5 | 0.12 | 62.2 | 0.49 | 6.77E+05 | 0.0016 | 60 |
| 30 | 6.1 | 0.19 | 52.1 | 0.55 | 9.10E+05 | 0.0014 | 110 |
| 35 | 5.1 | 0.26 | 43.9 | 0.62 | 1.21E+06 | 0.0012 | 180 |
| 40 | 4.3 | 0.33 | 37.5 | 0.71 | 1.58E+06 | 0.0012 | 310 |
| 46 | 3.5 | 0.42 | 31.4 | 0.83 | 2.11E+06 | 0.0017 | 740 |

* = full scale; ** = model scale; $v = 0.00001078$ ft²/sec (model tests)

4) Total Resistance Rt = RBAREHULL + Ra + Rws

| Vk | 20 | 25 | 30 | 35 | 40 | 46 |
|--------|------|------|------|------|------|------|
| Rt,lbs | 7050 | 6420 | 6060 | 6000 | 6260 | 7130 |

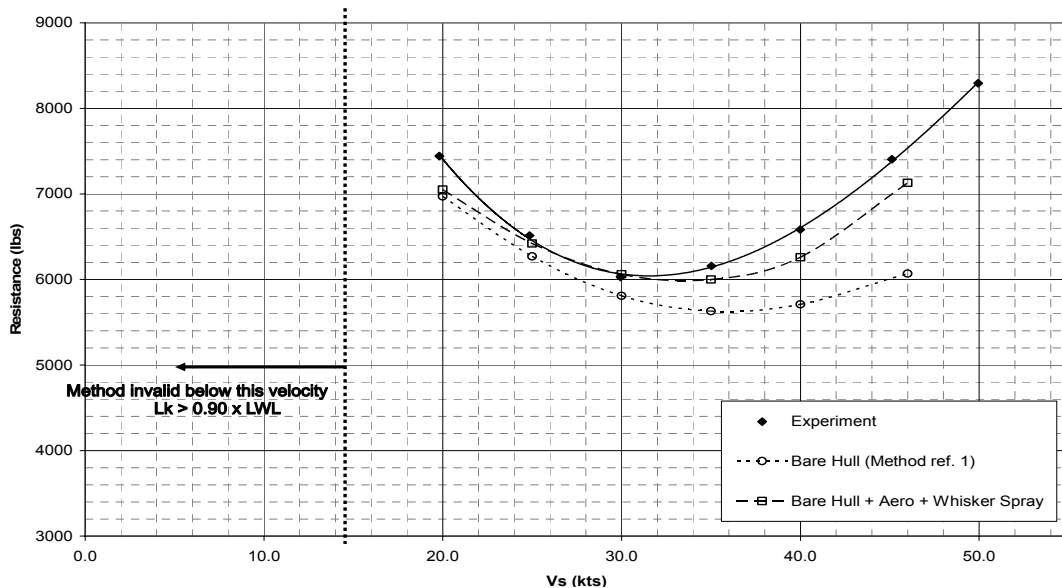
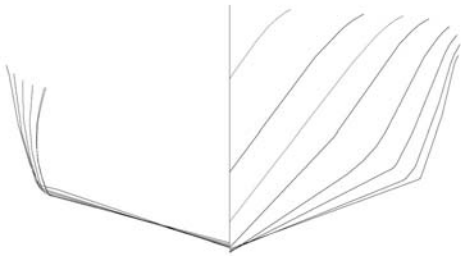


Table 3: Computed v. Experimental Total Resistance

(Model Scale = 16)



Geometry and Test Conditions

(Full Scale Values)

- Δ = 95,000 lbs
- LCG = 27.3 ft forward of transom
- Beam @ LCG = 16 ft
- Deadrise @ LCG = 19 deg
- Shaft angle = 14.4 deg
- Frontal area of hull above keel = 150 ft²
- LOA = 69.3 ft
- Roughness allowance = 0.0000

1) Bare Hull Resistance (Use method described in Ref 1)

| <u>Vk</u> | <u>V (ft/sec)</u> | <u>τ (deg)</u> | <u>Lk (ft)</u> | <u>Lc (ft)</u> | <u>RBARE HULL (lbs)</u> |
|-----------|-------------------|--------------------------------|----------------|----------------|-------------------------|
| 30 | 50.7 | 4.09 | 61.4 | 36.9 | 10570 |
| 32 | 54.1 | 4.06 | 59.7 | 35.0 | 10890 |
| 34 | 57.5 | 3.99 | 58.5 | 33.3 | 11160 |
| 36 | 60.8 | 3.89 | 57.6 | 31.8 | 11410 |

2) Aerodynamic Resistance = Ra (Use Equation 20):

| <u>Vk</u> | 30 | 32 | 34 | 36 |
|---------------|-----|-----|-----|-----|
| <u>Ra,lbs</u> | 320 | 360 | 400 | 450 |

$\rho_{air} = 0.00234 \text{ slugs/ft}^3$

3) Whisker Spray Resistance (Use Equation 13 and associated example)

| <u>Vk</u> | <u>τ</u> | <u>$\Delta\lambda$</u> | <u>2α</u> | <u>Lws**</u> | <u>RNws**</u> | <u>Cf**</u> | <u>Rws*</u> |
|-----------|--------------------------|-----------------------------------|-----------------------------|--------------|---------------|-------------|-------------|
| 30 | 4.1 deg | 0.36 | 36.1 deg | 0.45 ft | 5.27E+05 | 0.0018 | 410 lbs |
| 32 | 4.1 | 0.37 | 35.9 | 0.45 | 5.65E+05 | 0.0018 | 450 |
| 34 | 4.0 | 0.37 | 35.3 | 0.46 | 6.09E+05 | 0.0017 | 510 |
| 36 | 3.9 | 0.39 | 34.5 | 0.47 | 6.58E+05 | 0.0016 | 560 |

* = full scale; ** = model scale; $v = 0.00001078 \text{ ft}^2/\text{sec}$ (model tests)

4) Total Resistance $R_t = R_{BAREHULL} + R_a + R_{ws}$

| <u>Vk</u> | 30 | 32 | 34 | 36 |
|---------------|-------|-------|-------|-------|
| <u>Rt,lbs</u> | 11300 | 11700 | 12070 | 12420 |

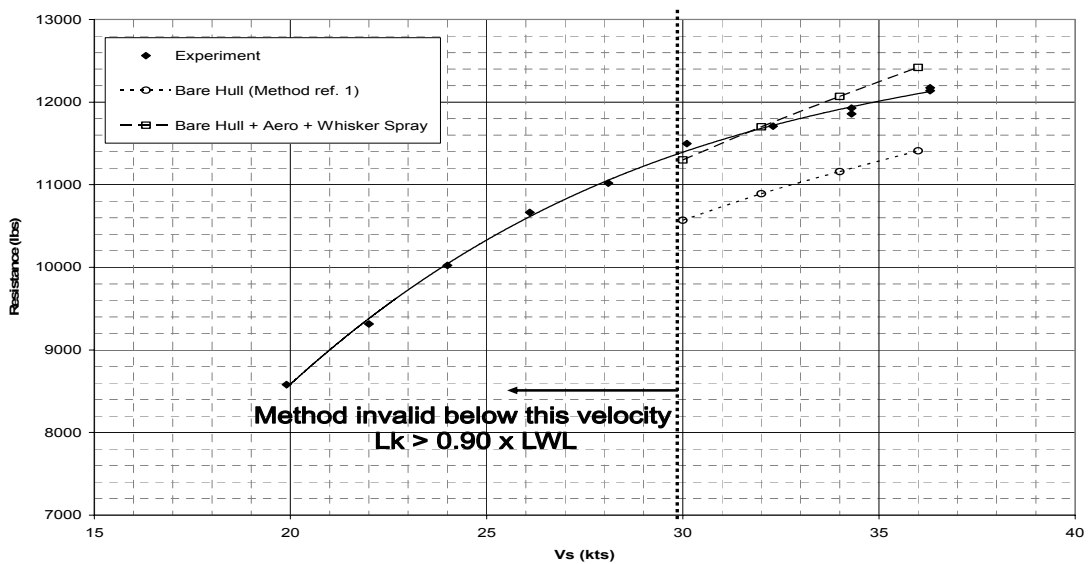
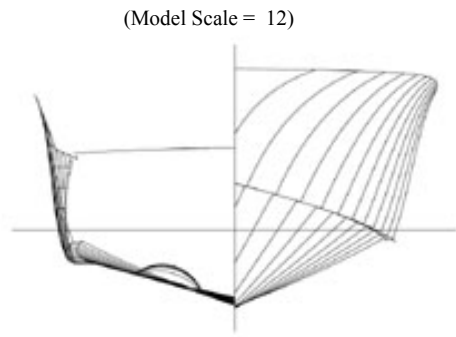


Table 4: Computed v. Experimental Total Resistance



Geometry and Test Conditions
 (Full Scale Values)
 $\Delta = 115,000$ lbs
 LCG = 27.5 ft forward of transom
 Beam @ LCG = 16.2 ft
 Deadrise @ LCG = 18.5 deg
 Shaft angle = 10 deg
 Frontal area of hull above keel = 164 ft²
 LOA = 74.5 ft
 Roughness allowance = 0.0004

1) Bare Hull Resistance (Use method described in Ref 1)

| <u>Vk</u> | <u>V (ft/sec)</u> | <u>τ (deg)</u> | <u>Lk (ft)</u> | <u>Lc (ft)</u> | <u>RBARE HULL (lbs)</u> |
|-----------|-------------------|--------------------------------|----------------|----------------|-------------------------|
| 30 | 50.6 | 4.82 | 58.6 | 38.2 | 14230 |
| 32 | 54.0 | 4.77 | 57.0 | 36.4 | 14580 |
| 34 | 57.4 | 4.67 | 55.8 | 34.8 | 14860 |
| 36 | 60.8 | 4.54 | 55.0 | 33.3 | 15120 |
| 38 | 64.1 | 4.39 | 54.4 | 32.0 | 15360 |
| 40 | 67.5 | 4.22 | 54.0 | 30.7 | 15620 |

2) Aerodynamic Resistance = Ra (Use Equation 20):

| <u>Vk</u> | 30 | 32 | 34 | 36 | 38 | 40 |
|---------------|-----|-----|-----|-----|-----|-----|
| <u>Ra,lbs</u> | 340 | 390 | 440 | 500 | 550 | 610 |

pair = 0.00234 slugs/ft³

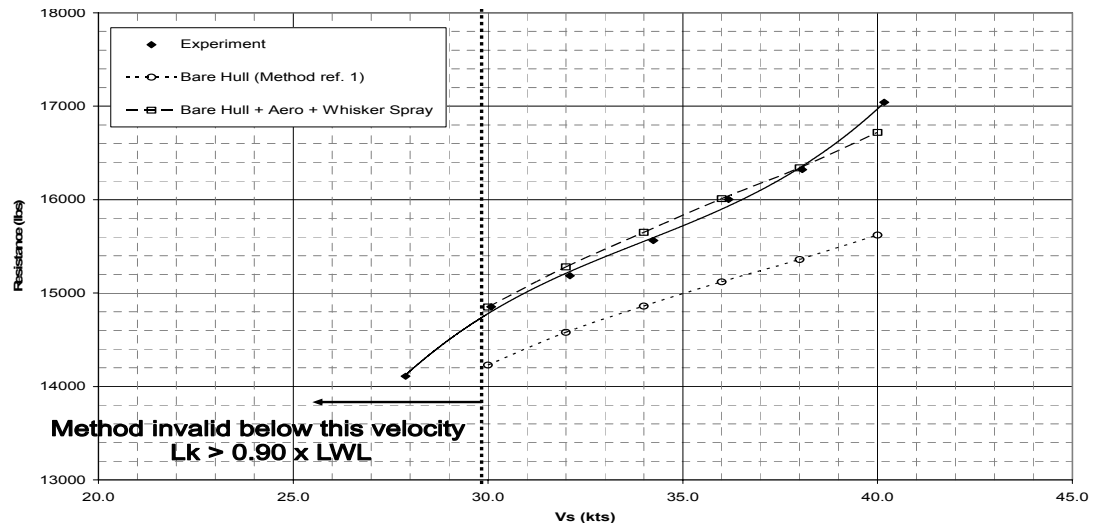
3) Whisker Spray Resistance (Use Equation 13 and associated example)

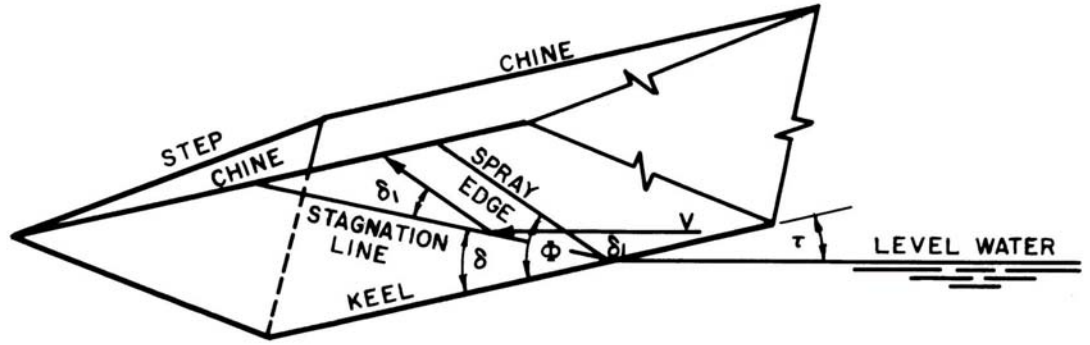
| <u>Vk</u> | <u>τ</u> | <u>$\Delta\lambda$</u> | <u>2α</u> | <u>Lws**</u> | <u>RNws**</u> | <u>Cf**</u> | <u>Rws*</u> |
|-----------|--------------------------|-----------------------------------|-----------------------------|--------------|---------------|-------------|-------------|
| 30 | 4.8 deg | 0.27 | 43.2 deg | 0.52 ft | 7.03E+05 | 0.0016 | 280 lbs |
| 32 | 4.8 | 0.27 | 42.8 | 0.52 | 7.56E+05 | 0.0015 | 310 |
| 34 | 4.7 | 0.28 | 42.0 | 0.53 | 8.15E+05 | 0.0015 | 350 |
| 36 | 4.5 | 0.29 | 40.9 | 0.54 | 8.82E+05 | 0.0014 | 390 |
| 38 | 4.4 | 0.31 | 39.6 | 0.56 | 9.55E+05 | 0.0014 | 430 |
| 40 | 4.2 | 0.33 | 38.2 | 0.57 | 1.04E+06 | 0.0013 | 490 |

* = full scale; ** = model scale; $v = 0.00001078$ ft²/sec (model tests)

4) Total Resistance Rt = RBAREHULL + Ra + Rws

| <u>Vk</u> | 30 | 32 | 34 | 36 | 38 | 40 |
|---------------|-------|-------|-------|-------|-------|-------|
| <u>Rt,lbs</u> | 14850 | 15280 | 15650 | 16010 | 16340 | 16720 |





$$\tan \theta = \tan \phi \cos \beta$$

$$\tan \alpha = \frac{\pi}{2} \frac{\tan \tau}{\tan \beta}$$

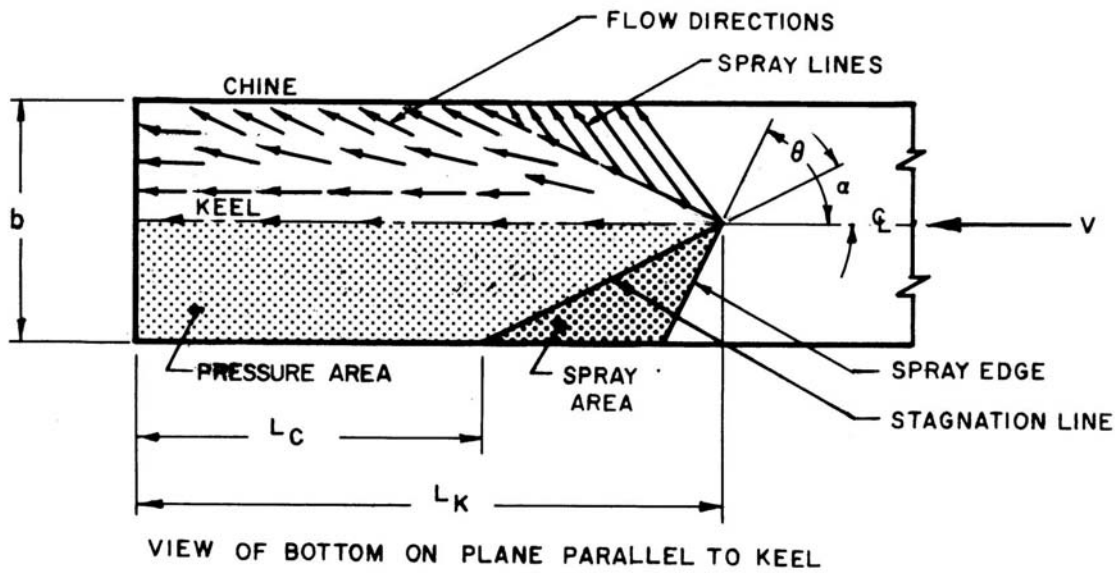


FIGURE 1: FLOW DIRECTION ALONG PLANING PRISM AND EXTENT OF SPRAY AREA.

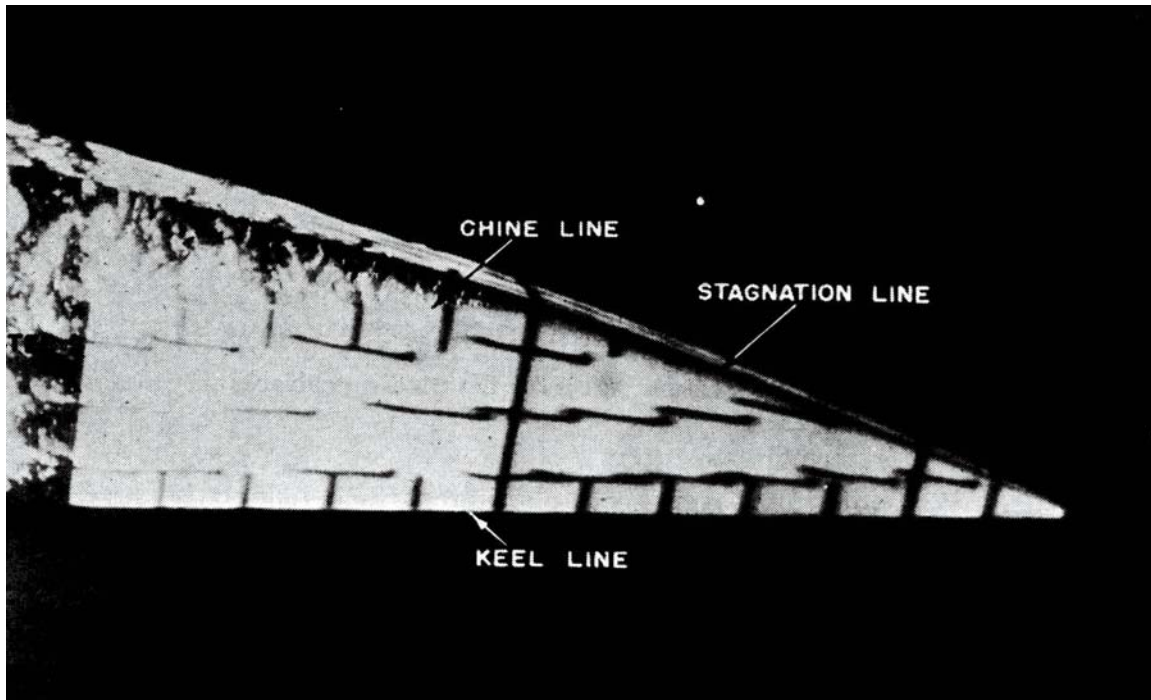


FIGURE 2: UNDERWATER PHOTOGRAPH SHOWING ARRANGEMENT OF TUFTS OVER BOTTOM ILLUSTRATING DIRECTION OF FLUID FLOW.

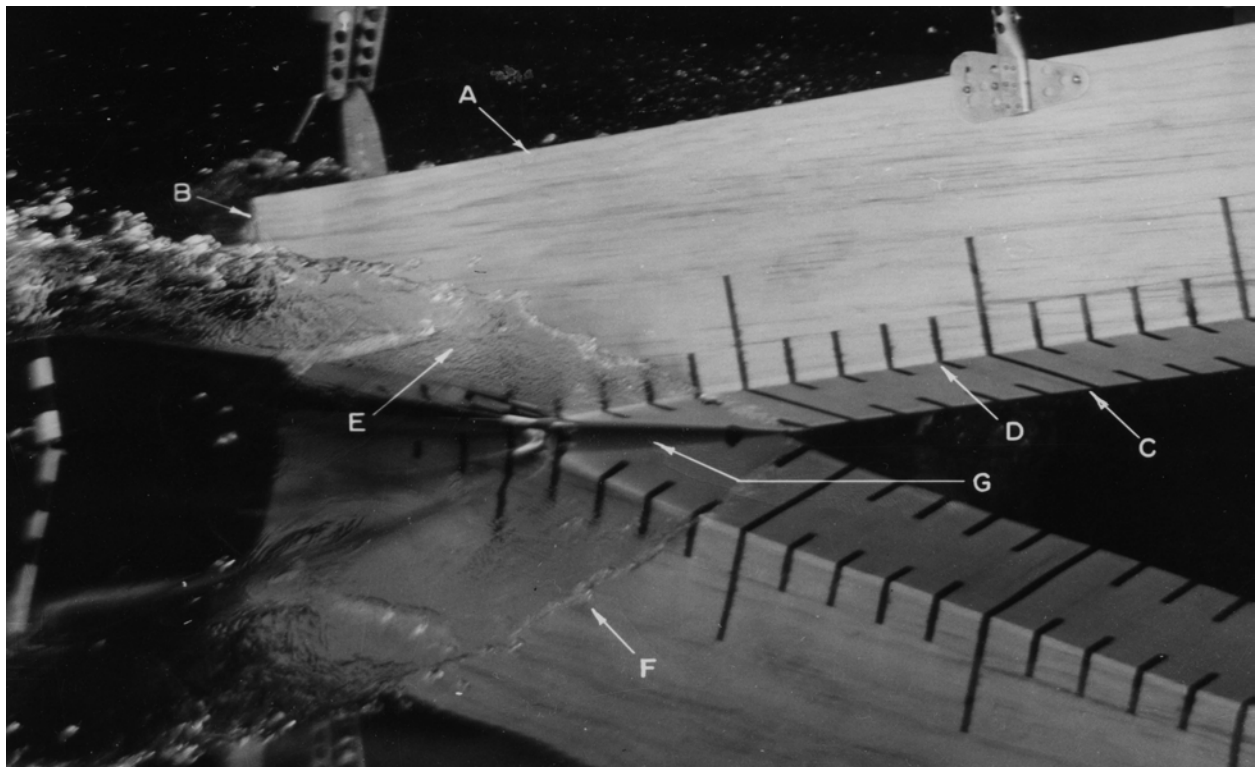


FIGURE 3: CHARACTERISTIC FEATURES OF VEE-BOTTOM PLANING SURFACE. A – MODEL OF WEDGE; B – TRANSOM; C – KEEL; D – CHINE; E – WHISKER SPRAY; F – REFLECTION OF SPRAY; G- SPRAY ROOT REGION.

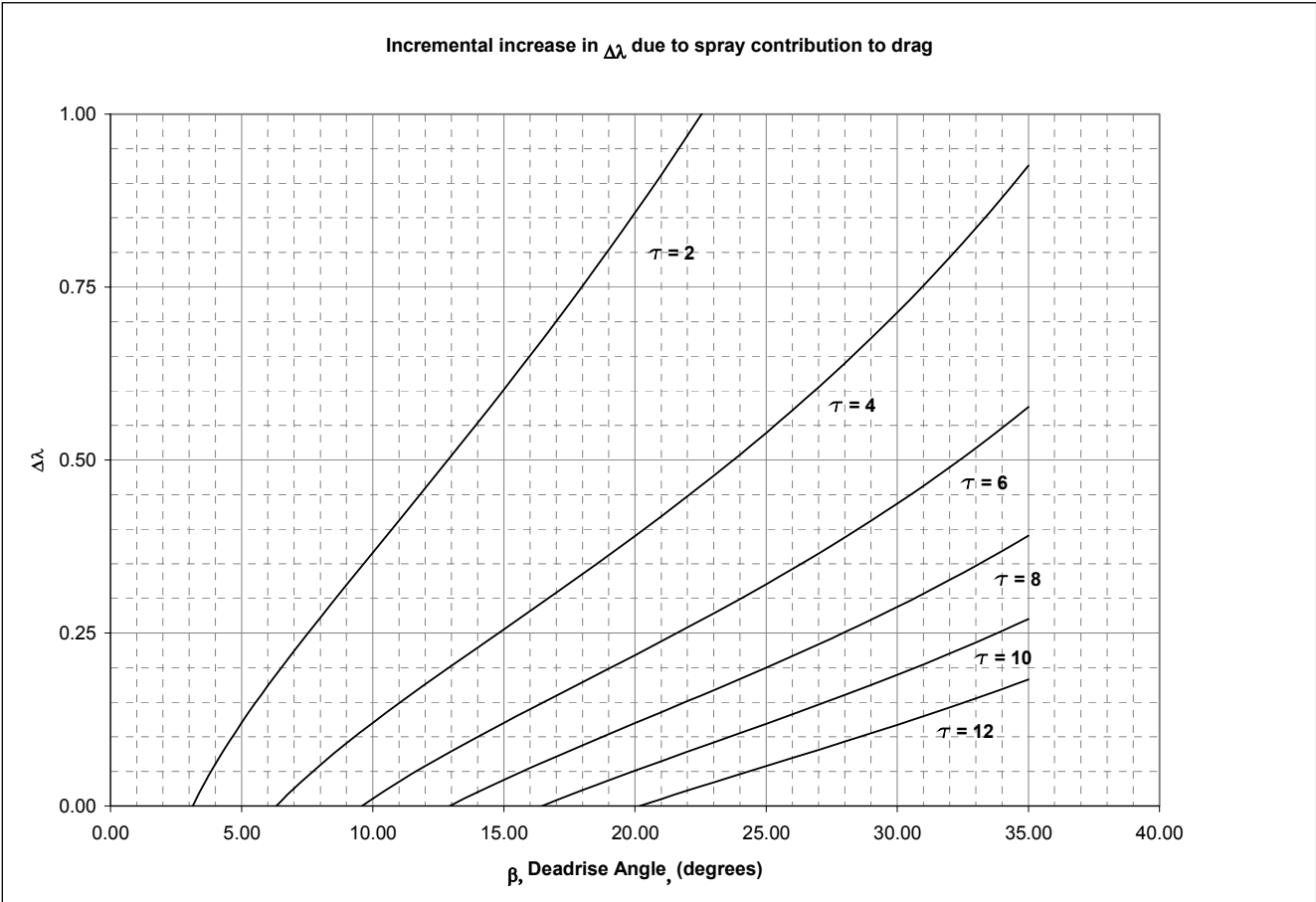


FIGURE 4: INCREMENTAL INCREASE IN $\Delta\lambda$ DUE TO SPRAY CONTRIBUTION TO DRAG.

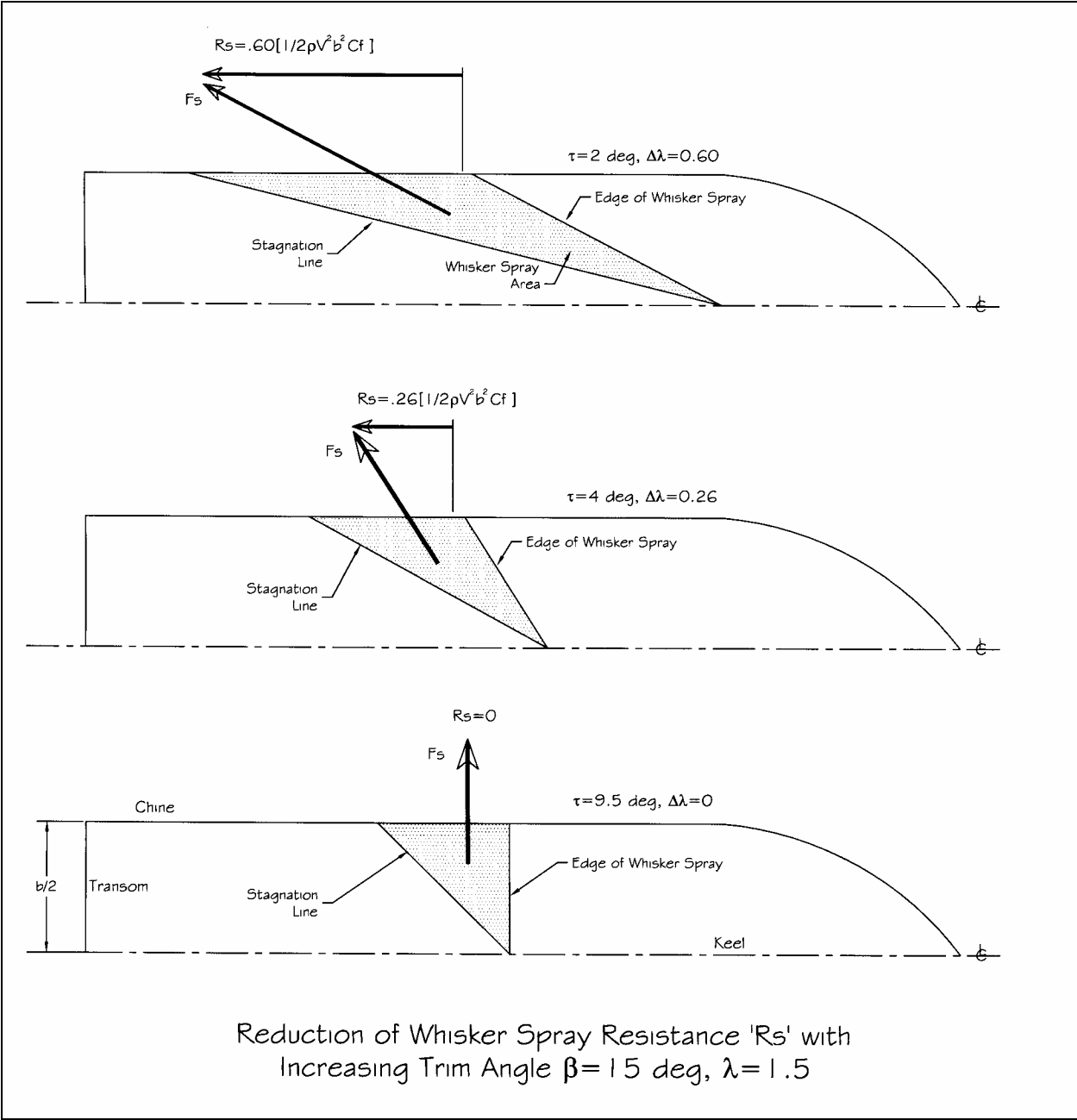


FIGURE 5: REDUCTION OF WHISKER SPRAY RESISTANCE WITH INCREASING TRIM ANGLE.

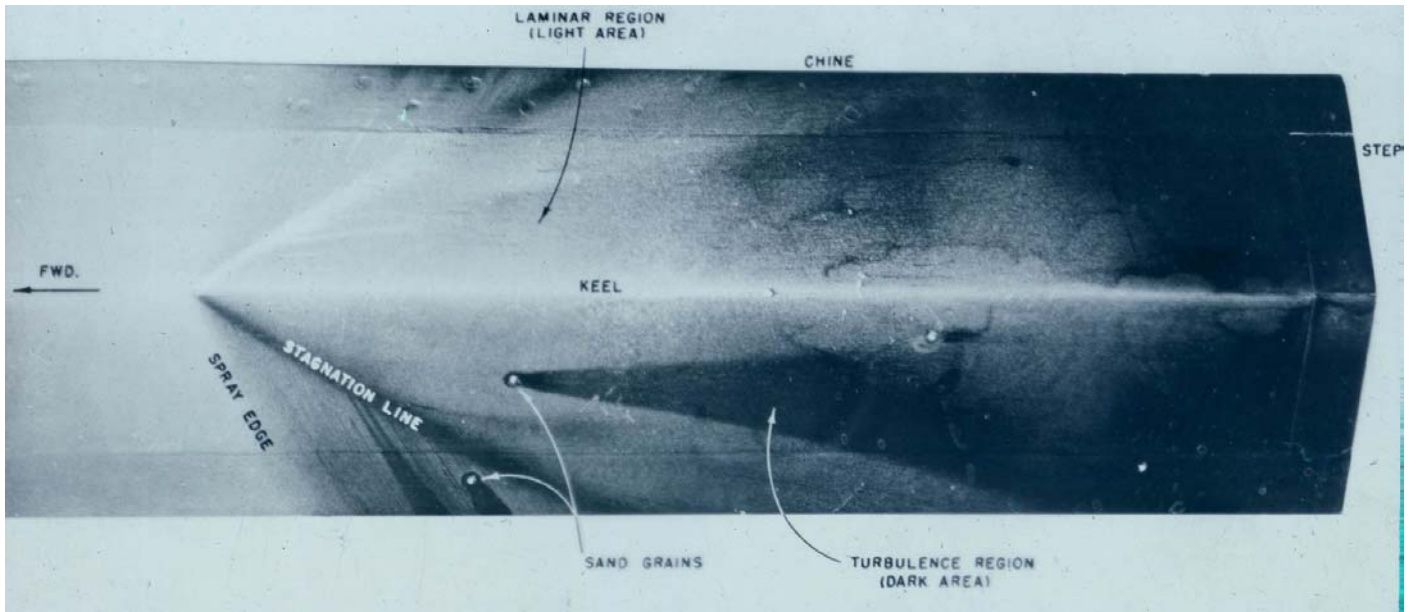


FIGURE 6: TYPICAL BOUNDARY LAYER PATTERN AFTER TEST RUN WITH CHEMICAL TURBULENCE DETECTION PAINT.

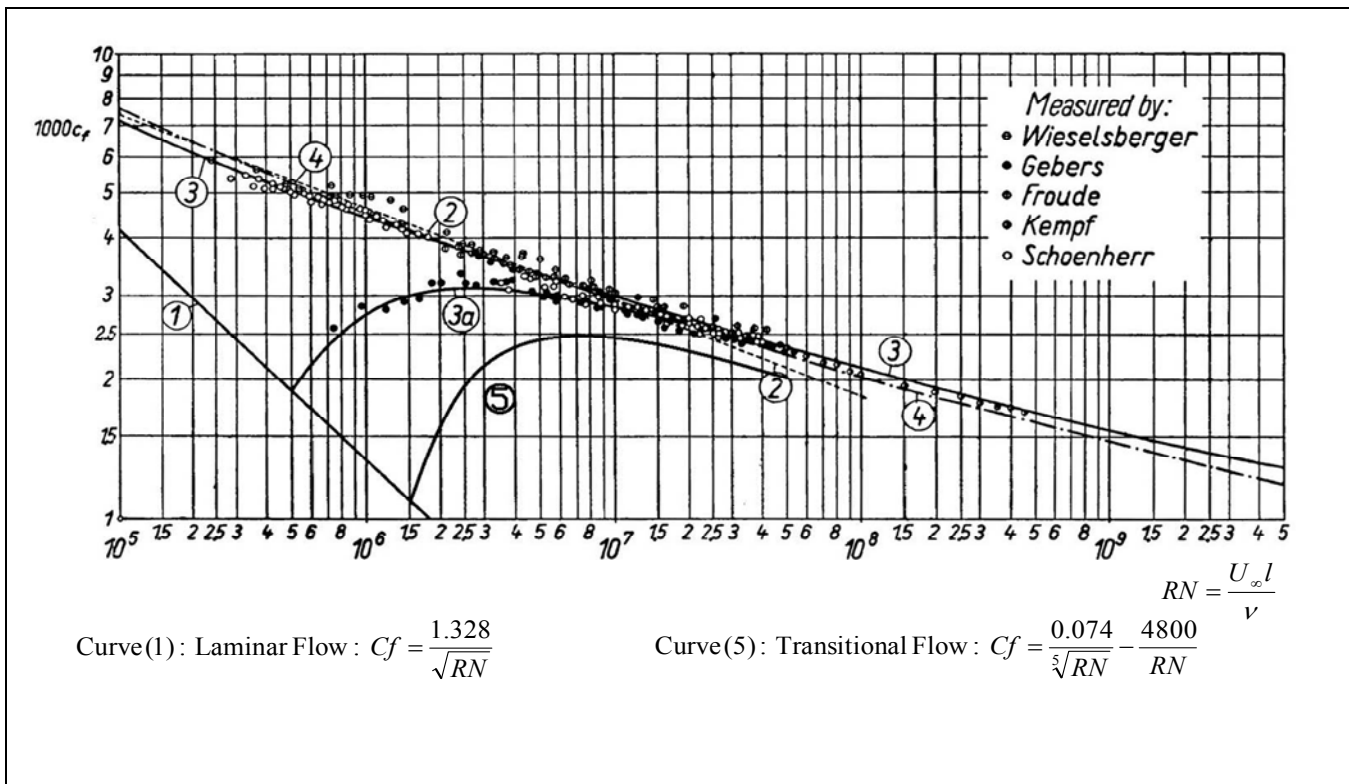


FIGURE 7: RESISTANCE FORMULA FOR SMOOTH FLATE PLATE AT ZERO INCIDENCE; COMPARISON BETWEEN THEORY AND MEASUREMENT (FROM SCHLICHTING REF. 6)

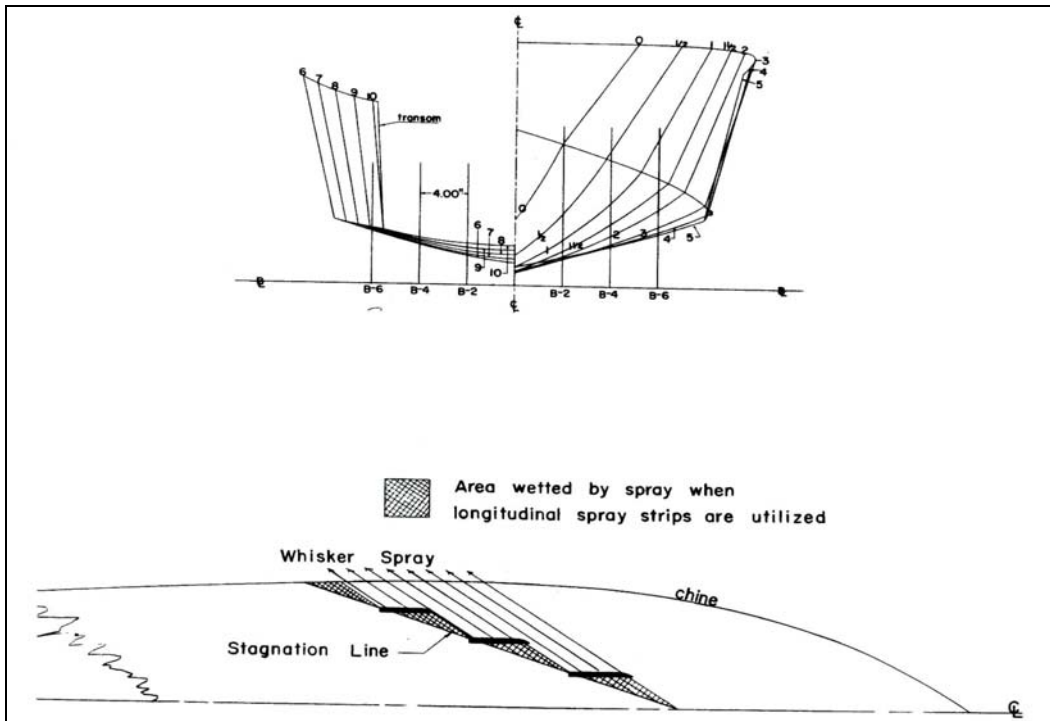


FIGURE 8: HULL BODY PLAN AND SHORT SPRAY STRIPS USED IN MODEL TESTS OF REFERENCE 2.

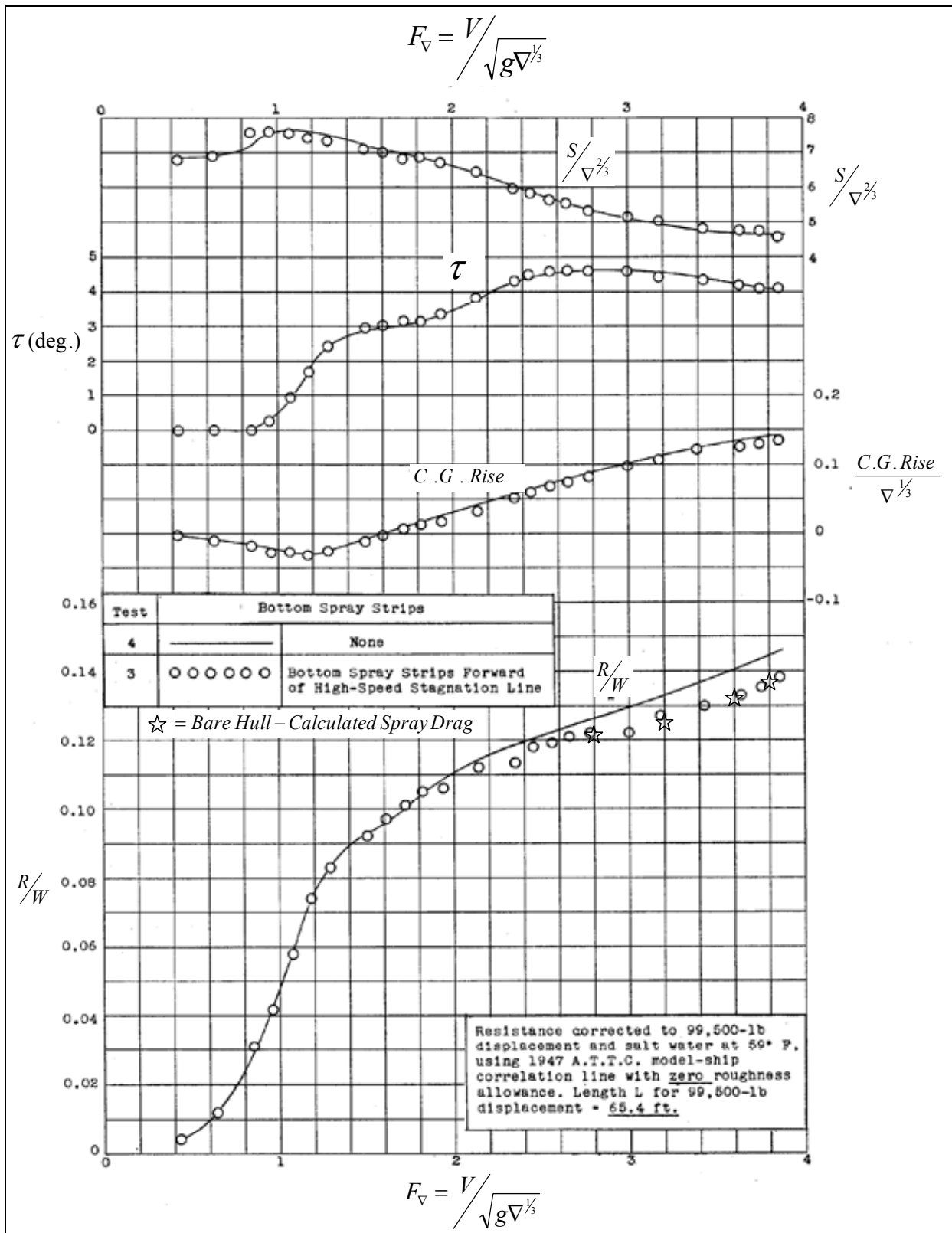


FIGURE 9: PERFORMANCE WITH NO BOTTOM STRIPS AND WITH SHORT SPRAY STRIPS (TAKEN FROM REF. 2) AND COMPARISON WITH SPRAY DRAG CALCULATED IN PRESENT STUDY.

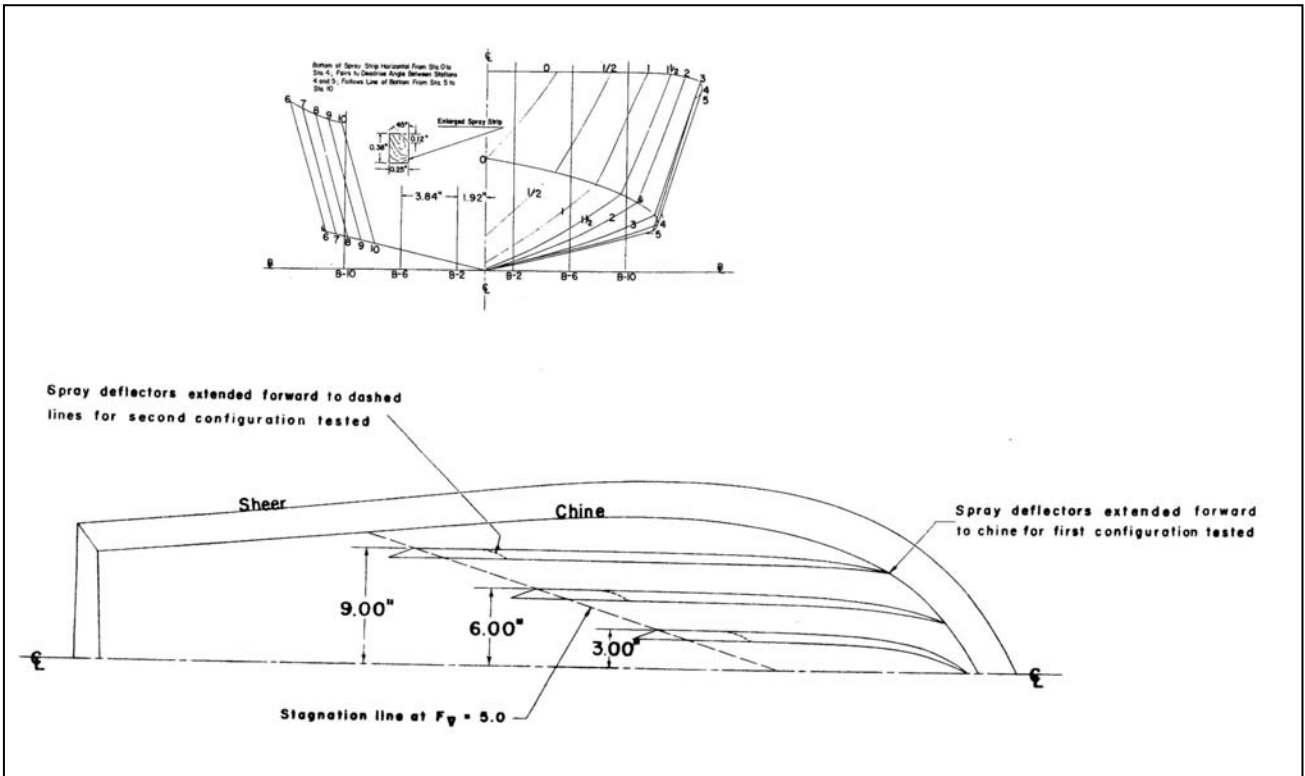


FIGURE 10: HULL BODY PLAN AND SPRAY STRIPS USED IN MODEL TESTS OF REFERENCE 3.

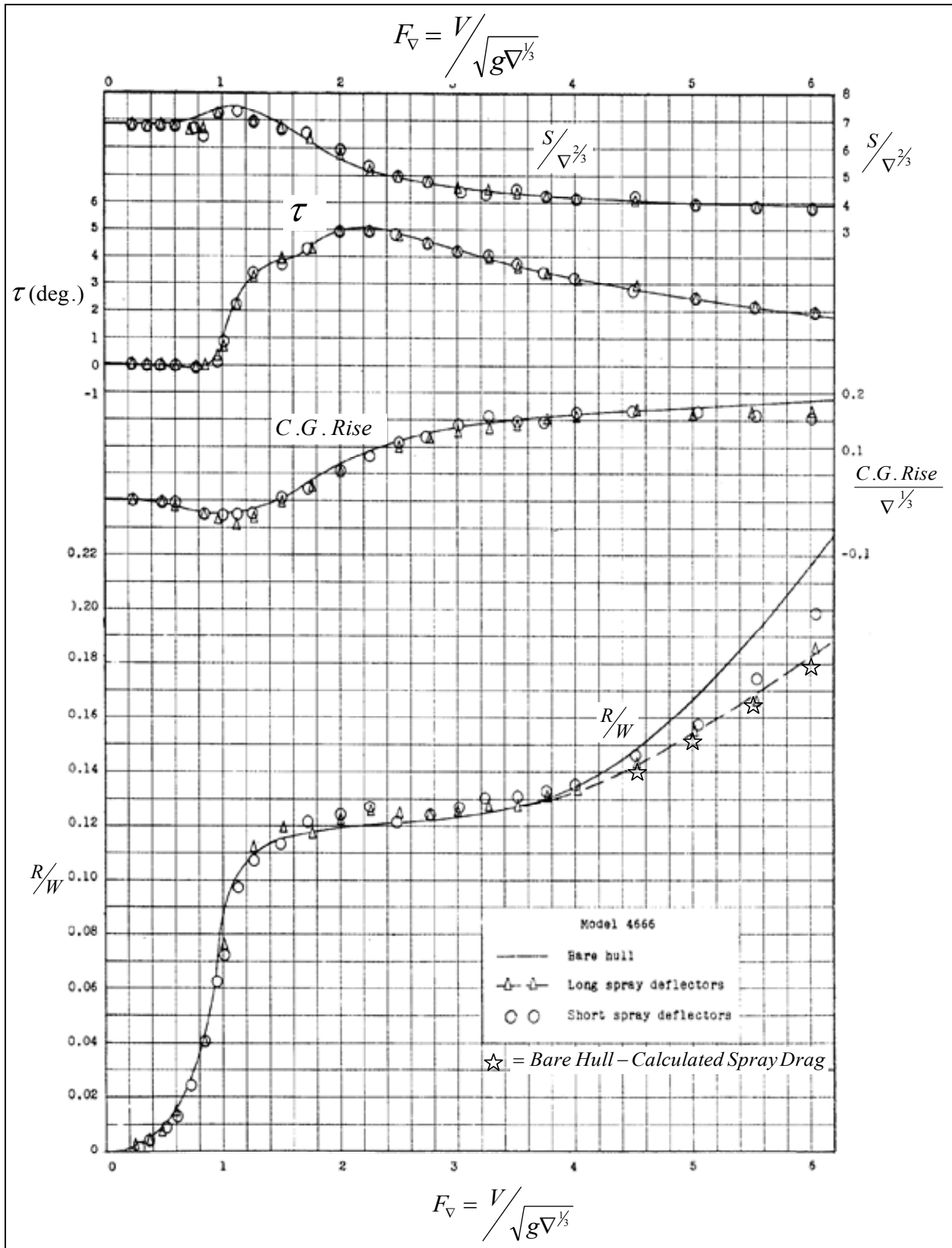


FIGURE 11: EFFECTS OF TWO CONFIGURATIONS OF SPRAY DEFLECTORS ON THE SMOOTH WATER PERFORMANCE OF A PLANING BOAT (TAKEN FROM REF. 3) AND COMPARED WITH SPRAY DRAG CALCULATED IN PRESENT STUDY.

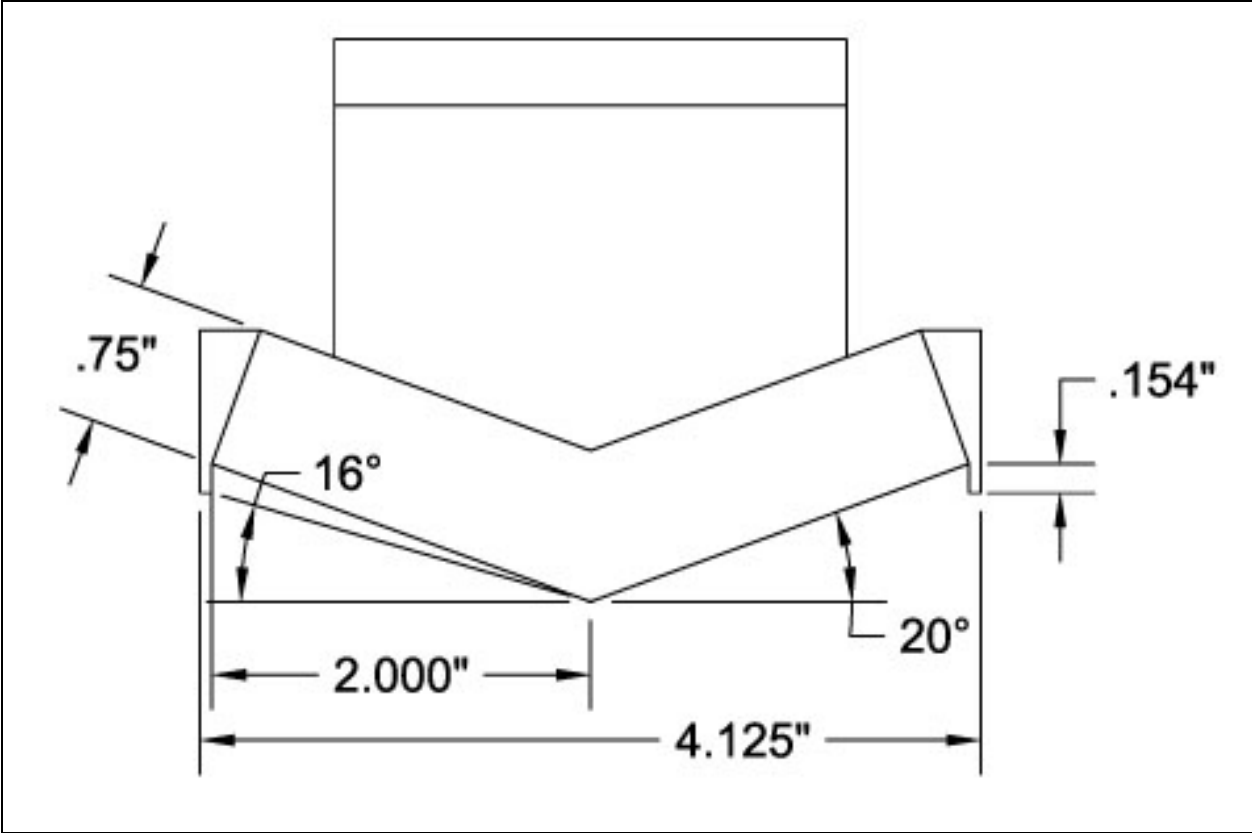


FIGURE 12: SKETCH AND CROSS SECTION OF LANGLEY MODEL 276B.

----- Calculated Friction Coefficient
Including Whisker Spray Drag

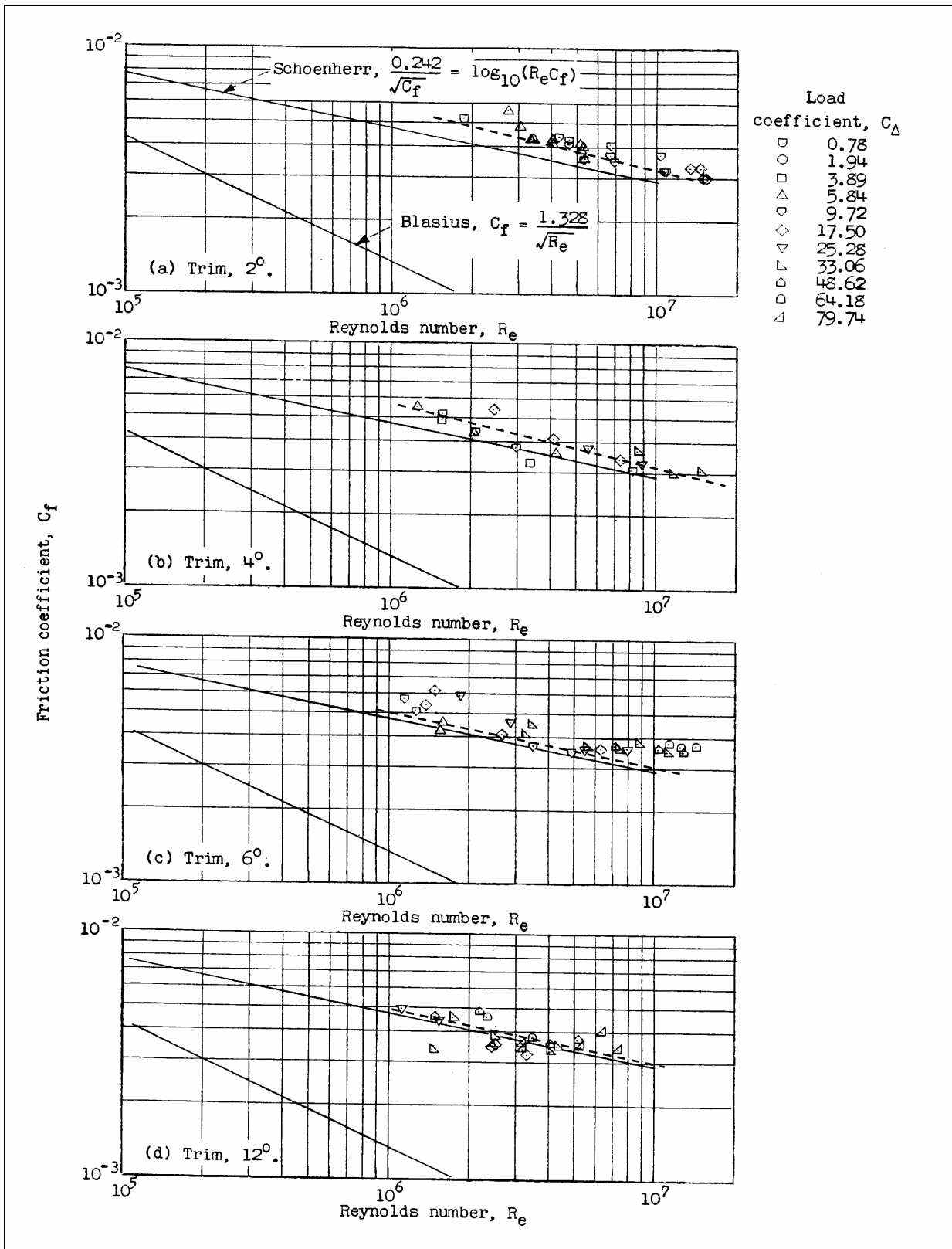


FIGURE 13: FRICTION DRAG COEFFICIENT VS. REYNOLDS NUMBER FOR TEST MODEL SHOWN ON FIGURE 12 (TAKEN FROM REF. 9)

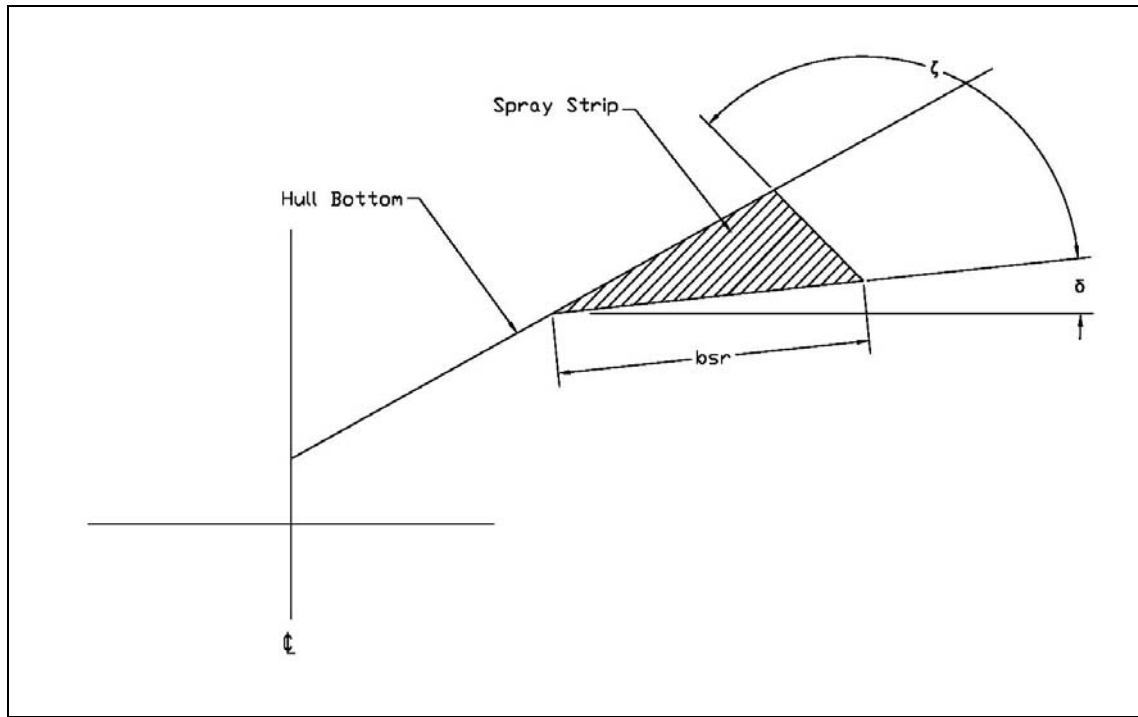


FIGURE 14: SUGGESTED SPRAY RAIL GEOMETRY (TAKEN FROM REF. 9)